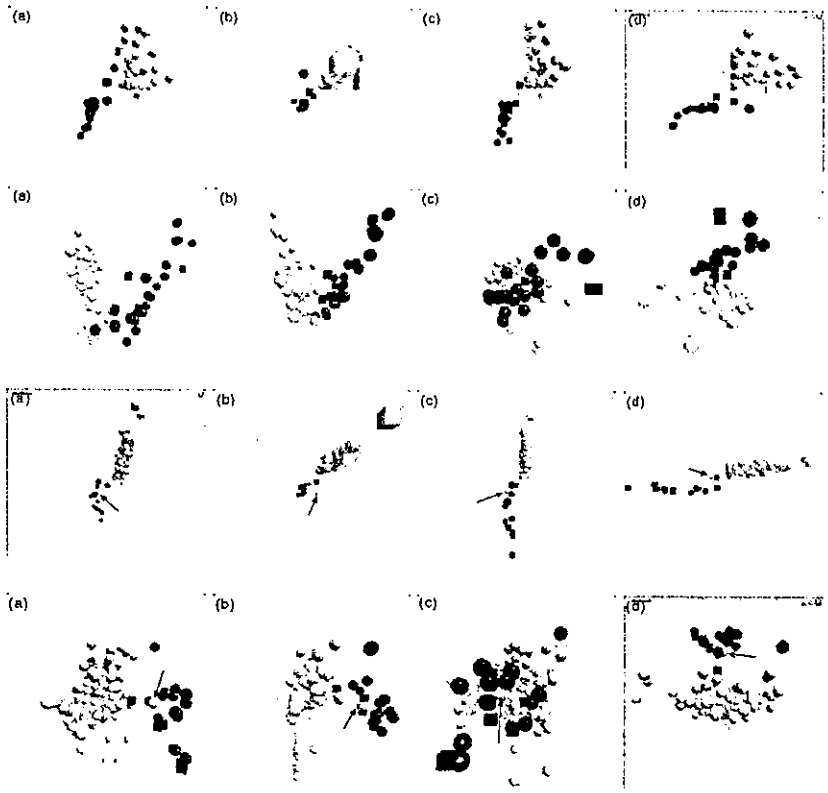

Fig. 1. (Top row) Distribution obtained by MD-SVMs for the leukemia dataset with linear kernel. (Second row) Distribution obtained by PCA on the leukemia dataset. (Third row) Distribution obtained by MD-SVMs for the lung tissues dataset with linear kernel. The sample indicated by arrows appears to be an outlier. (Fourth row) Distribution obtained by PCA for the lung tissues dataset. The sample indicated by arrows is the same as in the third row but with less deviates. (a) Cross shot, (b) 1st axis (x axis) and 2nd axis (y axis), (c) 2nd axis (x axis) and 3rd axis (y axis), (d) 3rd axis (x axis) and 1st axis (y axis). Black objects and white objects indicate AML samples (or normal tissues) ALL samples (or cancreous tissues), respectively. Training data and test data are expressed as a sphere and a cube, respectively.

Table 1. Number of classification errors in the MD-SVMs for the leukemia dataset. The columns 'n-th axis', $n = 1, 2, 3$, indicates the number of samples misclassified by n-th decision function. The columns 'n axes', $n = 1, 2, 3$, indicates the number of samples misclassified by n decision functions

Kernel	Sample	# of samples	1st axis	2nd axis	3rd axis	1 axis	2 axes	3 axes
Linear	Training	62	0	1	2	1	1	0
RBF	Training	62	0	2	7	5	2	0
Linear	Test	10	1	1	2	2	1	0
RBF	Test	10	0	2	0	2	0	0

Table 2. Number of classification errors in the MD-SVMs on the lung dataset. See the caption of Table 1 for other explanation

Kernel	Sample	# of samples	1st axis	2nd axis	3rd axis	1 axis	2 axes	3 axes
Linear	Training	170	0	1	1	0	1	0
RBF	Training	170	0	3	5	2	3	0
Linear	Test	33	1	0	0	1	0	0
RBF	Test	33	1	1	1	0	0	1

orthogonal axes, but it cannot predict classes of samples without other classification algorithms. We have tried to cover the shortcomings of both methods. MD-SVMs choose multiple orthogonal axes, which correspond to decision functions, from high dimensional space based on a margin between two classes. These multiple axes can be used for both visualization and class prediction.

Numerical experiments on real gene expression data indicate the effectiveness of MD-SVMs. All axes generated by MD-SVMs are taken into account for separating class of samples, while the 2nd and the 3rd axes by PCA are not. The samples in the distributions by MD-SVMs gather into appropriate clusters more vividly than those by PCA. MD-SVMs can predict the classes of the samples with multiple decision functions. We also indicate that MD-SVMs are useful for outlier detection with multiple decision functions.

There are several future works to be done on MD-SVMs: (1) application of our method to wider variety of gene expression datasets, (2) investigation of gene selection for preprocess of analysis and (3) investigation on class prediction method with multiple decision functions. Firstly, the use of more suitable samples may show that the axes chosen by MD-SVMs separate samples more clearly than those by PCA. Secondly, since the conventional SVMs show good generalization performance especially with large number of features, it is expected that MD-SVMs show much better performance than PCA with increasing the number of genes used in the numerical experiments. Since the element of weight vector generated by SVMs is one of the measures of discrimination power of the corresponding genes (Guyon *et al.*, 2002), that generated by MD-SVMs can be used for gene selection. Thirdly, the classification with probability as well as the weighted voting mentioned in Section 4 may be achieved in our scheme since the conventional SVMs have been already expanded for the purpose with sigmoid functions (Platt, 1999). We hope that our method sheds some lights on the future study of gene expression experiments.

REFERENCES

Bhattacharjee,A., Richards,W., Staunton,J., Li,C., Monti,S., Vasa,P., Ladd,C., Beheshti,J., Bueno,R., Gillette,M. *et al.* (2001) Classification of human lung carcinomas by mRNA expression profiling reveals distinct adenocarcinoma subclasses. *Proc. Natl Acad. Sci. USA*, **98**, 13790–13795.

Brown,M., Grundy,W., Lin,D., Cristianini,N., Sugnet,C., Furey,T., Ares,M. and Haussler,D. (2000) Knowledge-based analysis of microarray gene expression data by using support vector machines. *Proc. Natl Acad. Sci. USA*, **97**, 262–267.

Cristianini,N. and Shawe-Taylor,J. (2000) *An Introduction to Support Vector Machines and Other Kernel-based Learning Methods.* Cambridge University Press, NY.

Diamantaras,K. and Kung,S. (1996) *Principal Component Neural Networks Theory and Applications.* John Wiley & Sons, NY.

Fukunaga,K. (1990) *Introduction to Statistical Pattern Recognition.* Academic Press, NY.

Furey,T., Cristianini,N., Duffy,N., Bednarski,D., Schummer,M. and Haussler,D. (2000) Support vector machine classification and validation of cancer tissue samples using microarray expression data. *Bioinformatics*, **16**, 906–914.

Golub,T., Slonim,D., Tamayo,P., Huard,C., Gaasenbeek,M., Mesirov,J., Coller,H., Loh,M., Downing,J., Caligiuri,M., Bloomfield,C. and Lander,E. (1999) Molecular classification of cancer: class discovery and class prediction by gene expression monitoring. *Science*, **286**, 531–537.

Guyon,I., Weston,J., Barnhill,S. and Vapnik,V. (2002) Gene selection for cancer classification using support vector machines. *J. Machine Learn.*, **46**, 389–422.

Huang,E., Ishida,S., Pittman,J., Dressman,H., Bild,A., Kloos,M., D'Amico,M., Pestell,R., West,M. and Nevins,J. (2003) Gene expression phenotypic models that predict the activity of oncogenic pathways. *Nat. Genet.*, **34**, 226–230.

Khan,J., Wei,J., Ringnér,M., Saal,L., Ladanyi,M., Westermann,F., Berthold,F., Schwab,M., Antonescu,C., Peterson,C. and Meltzer,P. (2001) Classification and diagnostic prediction of cancers using gene expression profiling and artificial neural networks. *Nat. Med.*, **7**, 673–679.

Platt,J. (1999) *Probabilistic Outputs for Support Vector Machines and Comparisons to Regularized Likelihood Methods.* MIT Press, Cambridge, MA.

Schölkopf,B., Smola,A. and Müller,K. (1998) Non-linear component analysis as a kernel eigenvalue problem. *Neural Comput.*, **10**, 1299–1319.

Tibshirani,R., Hastie,T., Narasimhan,B. and Chu,G. (2002) Diagnosis of multiple cancer types by shrunken centroids of gene expression. *Proc. Natl Acad. Sci. USA*, **99**, 6567–6572.

Vapnik,V. (1998) *Statistical Learning Theory.* John Wiley & Sons, NY.

Carcinogenesis vol.25 no.8 pp.1495–1505, 2004
doi:10.1093/carcin/bgh155

Global gene expression analysis of rat colon cancers induced by a food-borne carcinogen, 2-amino-1-methyl-6-phenylimidazo[4,5-*b*]pyridine

Kyoko Fujiwara, Masako Ochiai, Tsutomu Ohta[1], Misao Ohki[1], Hiroyuki Aburatani[2], Minako Nagao, Takashi Sugimura and Hitoshi Nakagama[3]

Biochemistry Division and [1]Medical Genetics Division, National Cancer Center Research Institute, 5-1-1 Tsukiji, Chuo-ku, Tokyo 104-0045, Japan and [2]Research Center for Advanced Science and Technology, The University of Tokyo, 4-6-1 Komaba, Meguro-ku, Tokyo 153-8904, Japan

[3]To whom correspondence should be addressed. Tel: +81 3 3547 5239; Fax: +81 3 3542-2530;
Email: hnakagam@gan2.res.ncc.go.jp

Colon cancers develop after accumulation of multiple genetic and epigenetic alterations in colon epithelial cells. To shed light on global changes in gene expression of colon cancers and to gain further insight into the molecular mechanisms underlying colon carcinogenesis, we have conducted a comprehensive microarray analysis of mRNA using a rat colon cancer model with the food-borne carcinogen, 2-amino-1-methyl-6-phenylimidazo[4,5-*b*]pyridine (PhIP). Of 8749 genes or ESTs on a high density oligonucleotide microarray, 27 and 46 were over- and underexpressed, respectively, by ≥3-fold in colon cancers in common in two rat strains with distinct susceptibility to PhIP carcinogenesis. For example, genes involved in inflammation and matrix proteases and a cell cycle regulator gene, *cyclin D2*, were highly expressed in colon cancers. In contrast, genes encoding structural proteins, muscle-related proteins, matrix-composing and mucin-like proteins were underexpressed. Interestingly, a subset of genes whose expression is characteristic of Paneth cells, i.e. the *defensins* and *matrilysin*, were highly overexpressed in colon cancers. The presence of *defensin 3* and *defensin 5* transcripts in cancer cells could also be confirmed by *in situ* mRNA hybridization. Furthermore, Alcian blue/periodic acid Schiff base (AB-PAS) staining and immunohistochemical analysis with an anti-lysozyme antibody demonstrated Paneth cells in the cancer tissues. AB-PAS-positive cells were also observed in high grade dysplastic aberrant crypt foci, which are considered to be preneoplastic lesions of the colon. Our results suggest that Paneth cell differentiation in colon epithelial cells could be an early morphological change in cryptic cells during colon carcinogenesis.

Introduction

The development of colon cancers comprises multiple steps requiring the accumulation of genetic and epigenetic alterations in colon epithelial cells, and these changes further affect expression of a variety of downstream genes and may cause considerable changes in gene expression profiles in cancer cells as a consequence. Inactivation of the *adenomatous polyposis coli* (*APC*) gene, β-*catenin*, K-*RAS*, *SMAD2*, SMAD4, *p53* and mismatch repair genes by genetic alterations, for example, play key roles (1,2). Furthermore, alterations of gene expression profiles by perturbation of CpG island methylation in promoter regions and/or the histone acetylation/deacetylation status of chromatin also have a substantial impact on colon carcinogenesis (2).

Oral administration of 2-amino-1-methyl-6-phenylimidazo[4,5-*b*]pyridine (PhIP), one of the most abundant heterocyclic amines produced while cooking meat and fish (3,4), induces aberrant crypt foci (ACF) (5,6), putative preneoplastic lesions of the colon (7,8), in experimental animals within a short period and colon adenomas and adenocarcinomas after 1 or 2 years in rats, preferentially in males (9). A number of studies have revealed that PhIP-induced rat colon cancers resemble human neoplasms with regard to observed histological features and genetic alterations (10–14). There are several advantages with the use of animal cancer models to dissect the molecular basis of colon carcinogenesis. For example, inbred experimental animals share a common genetic background within the strain and, furthermore, carcinogenesis experiments using these animals can be carried out under well-controlled conditions. Genetic and/or epigenetic alterations in colon cancers induced in experimental animals are therefore expected to be more uniform compared with those in humans with diverse genetic backgrounds. Colon cancers induced by PhIP indeed demonstrate β-catenin accumulation in both cytoplasm and nucleus (13) and β-*catenin* mutations are observed at codons 32, 34, 36 or 38 in exon 2, the majority being G → T transversions (12,13). In the *Apc* gene, 5′-GGGA-3′ sites in exons 14 and 15 and a 5′-agGGGGG-3′ site at the junction of intron 10 and exon 11 are mutation hot-spots (10,13). Using a model system, we have recently revealed sequential progression from dysplastic ACF to colon cancer (14,15). Although the PhIP-induced rat colon cancer model has provided cancer researchers with a powerful tool for dissecting molecular events involved in the formation of colon cancers with relevance to human colon carcinogenesis, extensive studies aimed at the elucidation of early genetic events in colon cancer development have hitherto not been conducted.

In the present study we therefore performed a global gene expression analysis of rat colon cancers induced by PhIP using high density oligonucleotide microarrays (GeneChip; Affymetrix, Santa Clara, CA). To eliminate detection of strain-specific changes, but rather to detect specific gene expression profiles essential for colon cancer development, two rat strains, F344 and ACI, were subjected to analysis, the former being the more susceptible to PhIP-induced colon carcinogenesis. A considerable number of genes were found to be differentially expressed in colon cancers compared with normal counterpart epithelium, including examples characteristic of Paneth cells. Global

Abbreviations: AB-PAS, Alcian blue/periodic acid Schiff base; ACF, aberrant crypt foci; DIG, digoxigenin; APC, adenomatous polyposis coli; EST, expressed sequence tagged; H&E, hematoxylin and eosin; PhIP, 2-amino-1-methyl-6-phenylimidazo[4,5-*b*]pyridine.

changes in gene expression profiles are also discussed in comparison with those reported in human colon cancers. Another focus is on the appearance of Paneth cells in ACF, especially in dysplastic ones, and its biological significance.

Materials and methods

Animals and diets

PhIP was purchased from the Nard Institute (Osaka, Japan) in the form of PhIP-HCl and added to AIN-93G basal diet (7% w/w soybean oil; Dyets, Bethlehem, PA) at a concentration of 400 p.p.m. A high fat diet (AIN-93G basal diet supplemented with 23% w/w hydrogenated vegetable oil) was also purchased from Dyets. Five-week-old male F344 and ACI strain rats were purchased from CLEA Japan (Tokyo, Japan) and housed 3 per cage in an air-conditioned animal room with a 12 h light/dark cycle. Prior to the experiment, all the animals were acclimatized to the housing environment and the AIN-93G basal diet for 1 week.

Experimental protocol and tissue samples

Starting at the age of 6 weeks, rats were fed a diet containing PhIP following an intermittent PhIP feeding protocol (13). At experimental week 60 all animals were killed and colons were removed. When colon cancers with polypoid growth were detected by the naked eye, cancerous parts were resected with a razor blade, bisected and one half was embedded in O.C.T. compound (Tissue-Tek; Sakura Finetechnical Co., Tokyo, Japan), frozen and stored at −80°C until use for frozen section preparation and RNA extraction. The remaining halves were fixed in neutral 10% formalin overnight at 4°C and embedded in paraffin blocks according to standard procedures. Normal counterparts were collected from the surrounding normal parts of the colon and separately embedded in O.C.T. compound and samples were snap-frozen in liquid nitrogen and stored at −80°C until use for RNA extraction. In separate experiments using the intermittent PhIP feeding protocol, ACF were assayed at experimental weeks 18 and 25, after fixation of tissue in formalin and embedding in paraffin blocks as described above.

High density oligonucleotide microarray analysis

Twelve colon cancer tissues, six each from F344 and ACI rats, and 12 normal counterparts were collected by digging them out of frozen O.C.T. blocks using 18 gauge needles. Total RNA was extracted from ~1 mg of tissue with TRIZOL reagent (Invitrogen, Carlsbad, CA). Two of six colon cancer tissues from F344 rats, however, did not provide sufficient amounts of good quality RNA. The remaining four samples from F344 and six from ACI rats were subjected to the following experiments. cRNA was synthesized, labeled with biotin and hybridized to high density oligonucleotide microarrays, Rat Genome U34A (RG U34A; Affymetrix), as described previously. The average hybridization intensity for each array was scaled to 1000 to reliably compare multiple arrays. Prior to statistical analysis, genes were filtered according to the following criteria. For genes overexpressed in cancers, for example, they should have 'present (P)' or 'marginal (M)' calls in at least half of the colon cancer samples of the respective rat strains. For genes underexpressed in cancers, in contrast, they should have P or M calls at least in half of the normal counterpart samples. To assess statistical differences in gene expression between colon cancers and normal tissues, average signal intensity and standard variation were calculated for each group and GeneSpring 4.3 (Silicon Genetics, Redwood City, CA) was employed for the Mann–Whitney *U*-test. The significant *P* value was set at 0.05. Then, genes which were differentially expressed between cancer and normal tissue at ≥3-fold were selected and subjected to further analysis, including Venn diagrams, hierarchical clustering analysis, functional classification and comparison with expression profiles of human colon cancers. Permutation analysis was also carried out to assess the statistical significance of genes differentially expressed between the two rat strains.

Histological analysis

For hematoxylin and eosin (H&E) staining, paraffin sections were prepared at 3.5 μm thickness following standard procedures. Histological evaluation of colonic lesions was performed as described previously (13). For Alcian blue (pH 2.5)/periodic acid Schiff base (AB-PAS) staining to evaluate the presence of Paneth cells, both frozen (10 μm thickness) and paraffin (3.5 μm thickness) sections were used. The staining was carried out according to conventional methods.

In situ mRNA hybridiztion for defensin genes

In situ mRNA hybridization was carried out as described previously (16,17) under contract by Genostaff (Tokyo, Japan) using frozen sections prepared at 10 μm thickness. A 293 bp cDNA fragment of the rat neutrophil *defensin 3* gene was amplified by PCR with primers 5′-CTCCCTGCATACGCCAAAG-3′ (forward) and 5′-AACAGAGTCGGTAGATGCG-3′ (reverse) and a 335 bp cDNA fragment of the *defensin 5* gene with primers 5′-AACTTGTCCTCCTT TCTGCC-3′ (forward) and 5′-AACATCAGCATCGGTGGCC-3′ (reverse). Amplified fragments were cloned into pCRII (Invitrogen) and digoxigenin (DIG)-labeled RNA probes were generated by an *in vitro* transcription method using DIG-labeling mix (Roche Molecular Biochemicals, Tokyo, Japan). Hybridized probes were detected by an IgG antibody against the DIG label and visualized with NBT/BCIP solution (Roche Molecular Biochemicals). Nuclear counterstaining was performed with Kernechtrot Stain Sol (Muto Chemical, Tokyo, Japan).

Semi-quantitative RT–PCR

Extracted RNA was transcribed to cDNA using an oligo$(dT)_{12-18}$ primer and SuperScript™ II reverse transcriptase (Invitrogen) and the cDNAs produced were divided into aliquots in tubes and stored at −20°C until analyzed. Each aliquot of cDNA was subjected to semi-quantitative reverse transcription (RT)–PCR with the primer sequences listed in Table I. A set of semi-quantitative RT-PCR reactions for representative genes was carried out within 1 day to avoid the effects of degradation of cDNA templates. For reference, expression of the β-*actin* and *glyceraldehyde 3-phosphate dehydrogenase* (*G3PDH*) genes was also quantified for each sample. PCR amplification was carried out at 94°C for 30 s, 60°C for 30 s and 72°C for 1 min using Advantage Taq (Clontech, Palo Alto, CA) under the conditions recommended by the manufacturer. PCR cycles were set at 25 for β-*actin* and *G3PDH*, 35 for α-*defensin NP4* and β-*defensin 2* and 30 cycles for the other genes. PCR products were also analyzed by gel electrophoresis on a 2% agarose gel in 0.5× TBE (89 mM Tris, 89 mM boric acid, 1.9 mM EDTA). The amounts of PCR products were quantified by analysis performed on a Macintosh iBook G3 computer using the public domain NIH Image program (developed at the US National Institutes of Health and available on the Internet by anonymous ftp from zippy.nimh.nih.gov. or on floppy disk from the National Technical Information Service, Springfield, VA, part no. PB95-500195GEI). PCR reactions for individual genes were

Table I. List of primers used for RT-PCR

Gene name	Forward primer	Reverse primer
Matrilysin	5′-TTCGCAAGGGGAGATCACG-3′	5′-AACAGAAGAGTGACCCAGAC-3′
Mash2	5′-TTACCCATGCTGTCTAGTGC-3′	5′-AGTCCTCCAGCAGTTCAAGT-3′
Oct1A	5′-CCTTCATCATCCTGGTCAC-3′	5′-ATGAAGGGGGTGAAGATCC-3′
Carbonic anhydrase IV	5′-GGTAAACGAGGGCTTCCAG-3′	5′-TGAGACCTGAACACCTGGC-3′
AA799832	5′-GCGATCATGCCTTGCTTAAC-3′	5′-TTCCAGCGGCAGATGAAGG-3′
Defensin NP1 like	5′-TGCTGTTCAAGATTTACGCG-3′	5′-ACCTTGATAGCCGAATGCAGC-3′
Defensin NP3	5′-CTCCCTGCATACGCCAAAG-3′	5′-AACAGAGTCGGTAGATGCG-3′
Defensin α5	5′-AACTTGTCCTCCTTTCTGCC-3′	5′-AACATCAGCATCGGTGGCC-3′
Defensin NP4	5′-GACACTCACTCTGCTCATCA-3′	5′-ATGACAAATGGCTTCTTCTC-3′
Defensin β1	5′-CTTGGACGCAGAACAGATCA-3′	5′-AAACCACTGTCAACTCCTGC-3′
β-Actin	5′-GACTTCGAGCAAGAGATGGC-3′	5′-AGGAAGGAAGGCTGGAAGAG-3′
G3PDH	5′-TCATGACCACAGTCCATGCC-3′	5′-CTCAGTGTAGCCCAGGATGC-3′

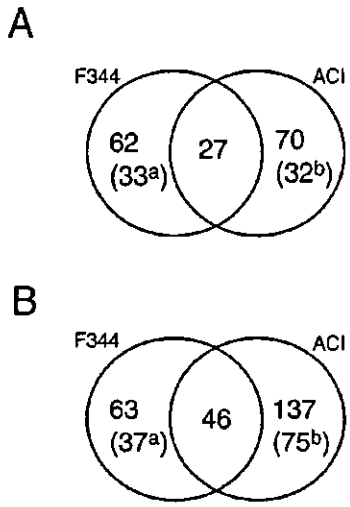

Fig. 1. Numbers of genes over- or underexpressed in colon cancers. Numbers of genes (A) overexpressed or (B) underexpressed in colon cancers of F344 or ACI rats are indicated in Venn diagrams. These genes showed significant differences ($P < 0.05$, Mann–Whitney U-test) between colon cancer tissues and normal colon tissues of ≥3-fold. The numbers in parentheses indicate the numbers of genes that also showed ≥2-fold differences in ACI (a) and F344 (b), respectively.

repeated twice, all of which gave similar results, and representative data are shown.

Results

Gene expression profiles in colon cancers of two rat strains

Of 8749 genes or ESTs on the RG U34A array, 89 and 97 were overexpressed ≥3-fold in colon cancers of F344 and ACI rats, respectively, and 109 and 183 were underexpressed by ≤3-fold, as shown in the Venn diagrams (Figure 1A and B; GeneChip data are available at http://www.ncc.go.jp/jp/nccri/divisions/02bioc/02bioc.html). As illustrated in Figure 1(A), 27 were overexpressed ≥3-fold in common in both F344 and ACI lesions. Although 62 genes were shown to be preferentially overexpressed in F344-derived colon cancers, 33 were also overexpressed ≥2-fold, in both strains (Figure 1A). Similarly, 32 of 70 genes overexpressed ≥3-fold in ACI rats were also overexpressed in the F344 strain by ≥2-fold. Collectively, of 159 genes which showed ≥3-fold expression in cancer tissues in either of the rat strains (Figure 1A), 92 (57.8%) showed ≥2-fold expression in colon cancers in both strains. Similarly, 158 of 246 (64.2%) genes demonstrated ≤2-fold expression in colon cancers in both strains (Figure 1B). We have recently reported that a considerable number of genes are differentially expressed in normal parts of colon epithelial cells between F344 and ACI rats after PhIP treatment (18) and the repertoire of differentially expressed genes may partly account for the different susceptibilities of the two rat strains. In contrast, differences in cancer tissues were relatively small compared with those in normal tissues. Permutation analysis was unable to detect apparent differences in the number of differentially expressed genes between cancer tissues of F344 and ACI rats, although significant differences were present in normal colon epithelium (data not shown). Hierarchical clustering analysis using the entire list of over- and underexpressed genes in cancers could not elucidate any cluster(s) of genes specific for either strain (data not shown).

Genes overexpressed in colon cancers

As described above, 27 genes were overexpressed ≥3-fold in common in both F344 and ACI rats (Figure 1A). Despite our efforts to elucidate meaningful signal pathways in those 27 genes using the bioinformatics software package GenMapp (http://www.genmapp.org/), none could be identified. This could be due, at least in part, to insufficient coverage of genes in signal pathway databases for rats. Manual classification, however, was able to elucidate some interesting tendencies. Genes involved in inflammation, such as those encoding *interleukin 1β*, *small inducible cytokine subfamily A20* precursor, and proteases, such as *matrilysin* (*Mmp7*) and *macrophage metalloelastase* (*Mme*) were highly overexpressed in cancer tissues (Table II). A cell cycle regulator, *cyclin D2*, and the cancer-related gene *retrotransposon virus-like 30s sequence* (*VL30*), which is known to be overexpressed in rodent hepatocellular tumors and lymphomas (19,20), were also highly expressed. Interestingly, a subset of genes encoding defensin and defensin-like proteins, which belong to the small cationic antimicrobial cytotoxic peptides (21–23), were overexpressed ≥10-fold. Differential expression of some of the representative genes was confirmed by semi-quantitative RT-PCR (Figure 2A).

Genes underexpressed in colon cancers

Forty-six genes were underexpressed ≤3-fold in common in colon cancers of both the F344 and ACI strains (Figure 1B). Genes encoding metabolic enzymes, such as alanine aminotransferase, minoxidil sulfotransferase and carbonic anhydrase IV, and signal transduction molecules were among the list (Table III). A considerable number of transcripts related to the structural proteins, i.e. skeletal and smooth muscle-related proteins, matrix-composing proteins and mucin-like proteins, were underexpressed in colon cancers. Down-regulation of mucin genes in colon cancers may reflect the drastic decrease in or complete loss of goblet cells in cancer tissues. Representative results of RT-PCR analyses are depicted in Figure 2A.

Expression of oncogenes and tumor suppressor genes

Expression of tumor-related genes, including those considered to be involved in colon carcinogenesis, was also evaluated utilizing the Chip data. Signals for the *Apc*, *bcl2*, c-*jun*, *erbB3*, *VHL* and *WT1* genes were below detectable levels. The *p53* and c-*fos* genes were expressed at comparable levels in both colon cancers and normal parts of colon tissues (data not shown). Only the c-*myc* gene was expressed at a significantly higher level in cancer tissues than in normal counterparts in both rat strains, with 4.0- and 2.5-fold differences in F344 and ACI rats, respectively.

Comparison of gene expression profiles with human colon cancers

Some of the genes in the list have already been reported to be either over- or underexpressed in human colon cancers (24,25). Average fold changes between colon cancers and normal counterparts were calculated using combined data from both the F344 and ACI strains and genes with ≥5-fold differences are listed in Table IV and compared with human cases, referring to the literature (24–31). The *defensin α5* and *defensin α6* genes were previously reported

Table II. Genes overexpressed in tumors of both F344 and ACI rats[a]

Gene name	Average signal intensity				Fold change (T/N)[b]	
	F344		ACI		F344	ACI
	Normal	Tumor	Normal	Tumor		
HLA and immune function genes						
Anti-acetylcholine receptor antibody gene, rearranged Ig Gamma-2a chain, VDJC region	246.73	3738.53	200.00	3929.67	15.15	19.65
Cytokines, inflammatory mediators, antimicrobial						
(EST) AI639089/similar to mouse defensin NP1 (α1)	1765.02	35820.01	200.00	55038.35	20.29	275.19
Defensin NP3 (α3) gene	898.73	14754.13	919.32	12107.13	16.42	13.17
Interleukin 1-β mRNA	200.00	1225.78	200.00	1658.88	6.13	8.29
Small inducible cytokine subfamily A20	573.80	2328.28	582.04	3176.26	4.06	5.46
Mob-1	214.46	758.60	200.00	979.33	3.54	4.90
Detoxification enzymes						
Glutathione *S*-transferase M5 (Gst-M5)	334.82	2013.20	259.33	1366.90	6.01	5.27
Protease and protease inhibitors						
Matrilysin (Mmp-7) mRNA	200.00	5823.69	200.00	15258.13	29.12	76.29
Macrophage metalloelastase (Mme)	200.00	2047.38	200.00	1990.87	10.24	9.95
Maspin	677.18	1954.74	637.72	2957.50	2.89	4.64
Ion transporters, carrier proteins						
Cation transporter Oct1A	1180.79	6642.65	756.38	6553.23	5.63	8.66
Intracellular calcium-binding protein Mrp14	200.00	1004.26	200.00	2011.03	5.02	10.06
Signal transduction molecules, transcription factor						
Mash-2 mRNA expressed in neuronal precursor cells	200.00	2867.48	303.83	3381.59	14.34	11.13
Platelet phospholipase A2	6078.53	54470.52	7630.13	99549.62	8.96	13.05
Receptor-linked protein tyrosine phosphatase	281.53	2171.51	200.00	2747.78	7.71	13.74
Inhibitor of DNA binding 3 (Idb3)	1585.27	7556.29	1819.98	9419.78	4.77	5.18
Hypertension-regulated vascular factor-1 (Ruk)	1956.67	7039.99	961.72	4728.72	3.60	4.92
Cell cycle regulators						
Cyclin D2	200.00	1281.43	200.00	1218.13	6.41	6.09
Similar to cyclin D2 (Vin1)	5132.35	19215.31	3399.26	18358.46	3.74	5.40
Cancer-related genes (function unknown)						
VL30 element	1055.79	10942.00	1234.52	6470.70	10.36	5.24
c-Ha-*ras* protooncogene mechanism sequence	4157.40	32175.09	2926.38	26356.43	7.74	9.01
Structural proteins						
Type I keratin (Mhr a-1)	200.00	3584.60	200.00	1440.44	17.92	7.20
β-Tubulin T β15	2176.01	8522.65	3252.25	11450.90	3.92	3.52
Serum protein						
α2-Macroglobulin	903.14	5880.35	1023.80	6303.21	6.51	6.16
Function unknown						
(EST) AA859937	572.42	5572.50	251.35	5924.12	9.73	23.57
(EST) AA799396	955.18	4061.69	1094.52	5774.63	4.25	5.28

[a]Genes with ≥3-fold difference compared with those in normal counterpart tissues are listed.
[b]Fold changes were calculated by dividing the signal intensity of colon cancer tissue by that of normal colon tissue.

to be up-regulated in human colon cancers [SAGE data (25)]. In the present study, *defensin NP3 (α3)* and *defensin NP1 (α1)-like molecule* were revealed to be overexpressed, although they have not been reported to be overexpressed in human cases. The matrix proteases *Mmp-7* and *Mme* [DNA chip data (24)] and *Mash2*, *Mrp14* and *cyclin D2* [SAGE data (25)] were also reported to be highly expressed in human colon cancers. In the case of underexpressed genes, many of them were also reported to be down-regulated in human cancers, such as *mucin*, *guanylin*, *carbonic anhydrase IV* and several muscle- and structure-related genes (24,32).

Expression of defensin family genes in rat colon cancers

Defensin genes are composed of mainly two families, α and β, categorized by sequence similarities (23,33). Genes in the former group are expressed mainly in neutrophils and some in the intestine, while the latter are ubiquitously expressed. *defensin NP1 (α1)-like molecule* and *defensin NP3 (α3)* was found to be highly expressed in colon cancers of both strains. *In situ* hybridization analysis revealed mRNAs of *defensin NP3 (α3)* and *defensin α5* to be expressed exclusively in epithelial cells of colon cancers and not expressed in matrix cells (Figure 3A). Normal epithelium did not show any positive signals. Overexpression of these genes in colon cancer tissues was confirmed by RT–PCR (Figure 2B). *defensin α5*, which is an intestinal-type defensin, but is not on the GeneChip, was also expressed exclusively in colon cancers. No expression was observed for *defensin NP4 (α4)*, *defensin β1* (Figure 2B) or *defensin β-2* (data not shown) in either cancers or normal counterpart tissues.

Presence of Paneth cells in cancers and preneoplastic lesions of the colon

Since intestinal-type defensins are known to be produced in Paneth cells (23,34), we examined the expression of other marker proteins specific to the Paneth cell lineage. H&E and

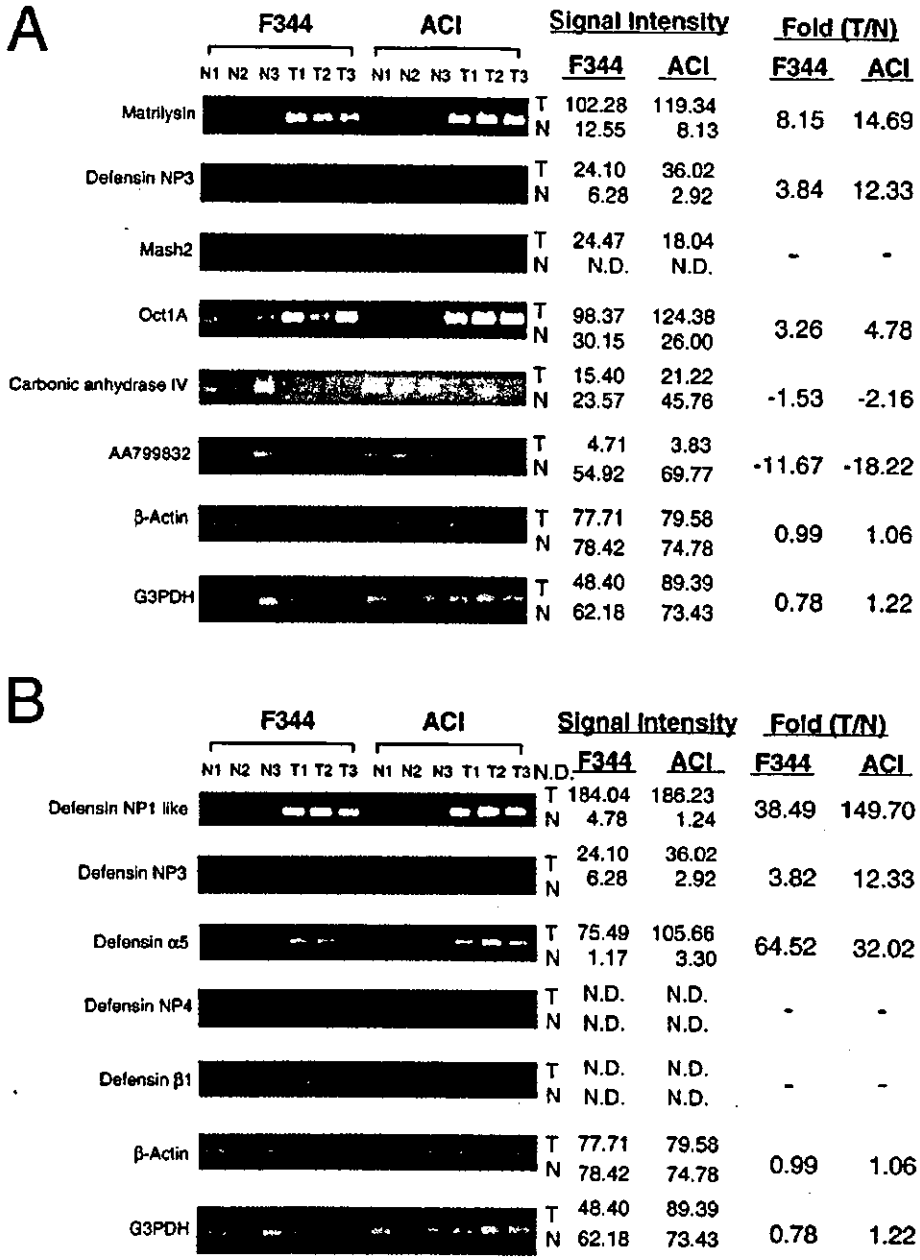

Fig. 2. Semi-quantitative RT-PCR analysis. (A) Among genes over- or underexpressed in colon cancers, expression levels of representative examples were confirmed by semi-quantitative RT-PCR analysis. Each lane indicates the gene expression level of either tumor or normal counterpart tissue from individual animals. The upper four panels illustrate higher expression of *matrilysin*, *defensin NP3*, *Mash2* and *Oct1A*, respectively, in cancer tissues (T_{1-3}) compared with normal epithelium (N_{1-3}). In contrast, *carbonic anhydrase IV* and *phosphoglucomutase 1* were underexpressed in cancers. Expression of β-*actin* and *G3PDH* was analyzed as an internal control. The amounts of PCR products were quantified by NIH image software. The signal values were calculated by subtracting blank values, which are average signal intensities of three different points outside the signal bands. Fold differences were calculated by dividing the average of the value of colon cancer tissues (T) by that of normal colon tissues (N). N.D. indicates a sample with no PCR product visible to the naked eye. (B) Expression levels of several *defensin* genes were analyzed by RT-PCR. *Defensin NP1-like molecule*, *defensin NP3*, *defensin 5* and *defensin NP4* are α-*defensin* family genes and *defensin β1* belongs to the β-*defensin* family gene. Quantification of the amounts of PCR products was carried out as above.

AB-PAS staining revealed the presence of Paneth granules in colon cancer cells and lysozyme expression was also observed in cells with Paneth granules (Figure 3B). Furthermore, Paneth cells were observed in adenomas and, to our surprise, even in preneoplastic lesions. When examined by H&E and AB-PAS staining, three of eight colon cancers and two of three high grade dysplastic ACF observed at 18 or 25 weeks were demonstrated to contain Paneth cells within the lesion (Figure 4A). None of the non-dysplastic ACF demonstrated Paneth cell differentiation (Figure 4B).

Table III. Genes underexpressed in tumors of both F344 and ACI rats[a]

Gene name	Average signal intensity				Fold change (T/N)[b]	
	F344		ACI		F344	ACI
	Normal	Tumor	Normal	Tumor		
Stress proteins and antioxidant						
Heat shock protein 27	8538.00	1967.31	11801.28	2648.38	4.34	4.46
Hsp70.2 mRNA for heat shock protein 70	766.00	200.00	3572.83	210.58	3.83	16.97
Metabolic enzymes						
Alanine aminotransferase mRNA	2078.57	200.00	1557.94	200.00	10.39	7.79
Minoxidil sulfotransferase	2170.13	208.88	1748.53	357.00	10.39	4.90
Carbonic anhydrase IV	2467.84	302.40	2651.28	220.07	8.16	12.05
Inducible carbonyl reductase	1676.98	234.19	1690.85	424.75	7.16	3.98
Skeletal muscle creatine kinase composite	1127.20	237.98	903.73	249.44	4.74	3.62
Mitochondrial 3-hydroxy-3-methylglutaryl-CoA synthase	8830.96	2414.46	9434.23	939.58	3.66	10.04
Monoamine oxidase B	680.05	200.00	918.93	200.00	3.40	4.59
Lipoprotein lipase	2259.29	684.09	2316.56	225.35	3.30	10.28
Protease						
Endopeptidase-24.18 α subunit	3327.41	773.59	5676.14	570.71	4.30	9.95
Ion transporters, carrier proteins						
SC1 protein	45395.45	3784.08	24395.65	1981.58	12.00	12.31
Dihydropyridine-sensitive L-type Ca^{2+} channel a-2 subunit	1420.65	229.11	3067.40	200.00	6.20	15.34
Guanylin	26005.42	5019.71	34049.06	6235.18	5.18	5.46
Growth factors and hormones						
Insulin growth factor-binding protein	2446.05	240.24	3255.07	200.00	10.18	16.28
Ebnerin	31568.63	3536.31	5773.52	1388.94	8.93	4.16
Signal transduction molecules, transcription factors						
Neuron-specific protein Pep-19	3125.96	200.00	2721.96	200.00	15.63	13.61
Phospholipase C-β1b	1714.75	244.15	2137.83	323.40	7.02	6.61
D-binding protein	1368.84	200.00	1038.96	200.00	6.84	5.19
Guanylate cyclase 1, soluble, α3	2375.39	384.13	1670.49	519.78	6.18	3.21
Gap-43 gene	1666.24	271.56	982.00	293.22	6.14	3.35
Ssecks 322	6158.29	1093.83	3320.23	522.72	5.63	6.35
N-myc downstream regulated 2	2273.34	486.21	3961.73	710.56	4.68	5.58
Tc10-like rho GTPase	2287.18	582.64	4295.60	511.18	3.93	8.40
BTE-binding protein	2136.52	625.70	3136.92	668.54	3.41	4.69
Structural proteins						
H36-α7 integrin α chain	11056.70	501.93	4844.89	392.89	22.03	12.33
α-Crystallin B chain	4016.12	200.00	3133.37	383.01	20.08	8.18
α b-Crystallin-related protein	4322.27	375.25	3731.25	200.00	11.52	18.66
Mucin-like protein	85858.60	26168.84	85879.95	15703.47	3.28	5.47
Muscle-related proteins						
Skeletal muscle β-tropomyosin and fibroblast tropomyosin 1	15036.62	578.13	8208.40	331.54	26.01	24.76
Myosin regulatory light chain isoform C	32928.30	1592.13	21440.35	576.02	20.68	37.22
γ-Enteric smooth muscle actin isoform	107504.58	5932.44	64435.47	1234.91	18.12	52.18
Calponin	22307.16	1283.39	14767.63	349.48	17.38	42.26
SM22 mRNA	25962.76	1742.56	9714.69	200.00	14.90	48.57
Alternatively spliced smooth muscle myosin heavy chain	21642.04	1629.01	13526.24	591.39	13.29	22.87
Vascular α-actin	28016.47	4213.15	28042.35	2126.16	6.65	13.19
Function unknown						
(EST) AA799832/similar to mouse phosphoglucomutase 5	17333.24	629.26	16572.28	200.00	27.55	82.86
(EST) AA799773/similar to mouse C3H filamin	4300.66	387.96	5571.79	558.87	11.09	9.97
(EST) AA800735/similar to archvillin	3155.42	366.63	3353.20	360.25	8.61	9.31
(EST) AA799580	2256.37	338.94	1619.85	420.47	6.66	3.85
(EST) AA799734	1290.58	200.00	950.38	200.00	6.45	4.75
(EST) AA892888	5611.57	949.04	3961.43	200.00	5.91	19.81
zymogen granule protein (Zg-16p)	14971.90	2743.63	25128.90	1816.38	5.46	13.83
(EST) AA893743/similar to human hox B2	1017.45	200.00	952.02	200.00	5.09	4.76
(EST) AI639501/similar to human brain cell membrane protein 1	4324.68	871.69	4080.30	1027.55	4.96	3.97

[a]Gene with ≥3-fold difference compared with those in normal counterpart tissues are listed.
[b]Fold changes were calculated by dividing the signal intensity of normal colon tissues by that of colon cancer tissues.

Discussion

With the present comprehensive gene expression analysis, conducted using PhIP-induced rat colon cancers in two rat strains, PhIP-induced colon cancers were found to possess somewhat common gene expression profiles in both F344 and ACI rats, despite the significant differences in gene expression between their normal colon epithelium (18). Furthermore, a subset of genes known to be overexpressed in

Table IV. Comparison of overexpressed and underexpressed genes in tumors of rat and human

Gene name	Rat	Human		
	Fold	DNA chip[a]	SAGE[b]	Other data
Overexpressed				
Defensin NP1 (α1)-like protein	53.30	Unchanged		
Matrilysin (Mmp-7) mRNA	41.89	8.00		Overexpressed (26,27)
(EST) AA859937	14.37	[c]		
Defensin NP3 (α3) gene	13.47	Unchanged		
Platelet phospholipase A2	12.02	Unchanged		Overexpressed (28)
Type I keratin (Mhr a-1)	9.86	[c]		
Anti-acetylcholine receptor antibody gene	9.63	[c]		
Mash-2 mRNA expressed in neuronal precursor cells	9.62	[c]	9/0	
c-Ha-*ras* protooncogene mechanism sequence	8.90	[c]		
Intracellular calcium-binding protein Mrp14	8.18	Unchanged	11/0	
Receptor-linked protein tyrosine phosphatase	8.06	[c]		
Macrophage metalloelastase (Mme)	7.45	5.10		
Cation transporter Oct1A	7.43	[c]		
VL30 element	6.75	[c]		
Interleukin 1-β mRNA	6.05	Unchanged		
Cyclin D2	5.60	Unchanged	8/0	Overexpressed (29)
α2-Macroglobulin	5.55	[c]		Overexpressed (30)
Under-expressed				
(EST)AA799832	40.36	2.7		
H36-α7 integrin α chain	15.58	2.8		
Neuron-specific protein Pep-19 mRNA, complete cds	13.61	2.1		
Scl protein	12.18	4.5		Underexpressed (31)
Zg-16p	11.35	[c]		
α b-crystallin-related protein	11.34	[c]		
Dihydropyridine-sesitive L-type calcium channel	10.42	Unchanged		
α-Crystallin B chain	10.19	4.3		
(EST)AF119148/Musmus C3H filamin	9.56	5.8		
Alanine aminotransferase mRNA	9.35	[c]		
Insulin growth factor-binding protein	9.28	1.6		
(EST)AA892888	7.77	[c]		
Carbonic anhydrase IV	7.68	2		
(EST) AA800735/similar to mouse Supervillin	7.16	[c]		
Guanylin	6.04	20	55/0	
Phospholipase C-β1b	5.78	[c]		
Ssecks 322	5.68	[c]		
D-binding protein	5.05	[c]	8/0	

The values indicate tag counts of normal tissues/tumor tissues.
[a]Data from Notterman *et al.* (24). Values indicate fold difference (normal/tumor).
[b]Data from Buckhaults *et al.* (25) and on-line SAGE database to which they submitted their results.
[c]There is no information in Notterman *et al.* (24) about these genes.

human colon cancers was highly expressed in colon cancers of both rat strains. In addition, there are substantial similarities in a list of underexpressed genes between human (24) and rat tumors (present study). The histological features of the rat cancers also showed a high similarity with human cases, as described previously (10,11,13,14). Taking all the data together, the PhIP-induced colon carcinogenesis model in rats thus appears an appropriate and relevant system for investigation of human colon carcinogenesis.

High expression of *cyclin D2* and c-*myc* may result from activation of the Wnt/β-catenin signaling pathway as a consequence of β-catenin accumulation, this being a common feature in rat and human tumors (2,13,35). An mRNA species for a mucin-like protein, homologous to mouse mucin 2, was here shown to be underexpressed in cancer tissues. Mucins are known to be abnormally expressed in neoplastic lesions of the colon of humans (36). Moreover, since *mucin* $2^{-/-}$ mice demonstrated reduced numbers of goblet cells and spontaneously developed adenomas in the small intestine (37), down-regulation of the mucin-like protein mRNA may play an important role in PhIP colon carcinogenesis in rats.

Some of the genes found in the present study, including those encoding helix–loop–helix protein MASH2, organic cation transporter (OCT1A4), calcium-binding protein MRP14 and regulator of ubiquitous kinase (RUK), have not been reported so far to be differentially expressed in human colon cancers. Some of them are intriguing with regard to their biological functions, although there are few reports suggesting their involvement in human colon carcinogenesis. Considering the size (small), the non-invasive nature of rat lesions and the rare occurrence of *p53* or K-*ras* mutations in PhIP-induced colon cancers (38,39), differential expression of these genes in cancer tissues may suggest that their alteration occurs at an early stage of human colon carcinogenesis. Alternatively, of course, this could simply be a rodent-specific phenomenon. Further analysis is warranted in the future to clarify this point.

Snyderwine *et al.* recently reported gene expression profiles in PhIP-induced mammary gland tumors (40). Expression of a few genes overlapped between mammary gland (40) and colon tumors (present study) induced by PhIP, except for the *tubulin β15* gene. In PhIP-induced rat mammary cancer, deregulation of cyclin D1/Cdk4 and phospho-Rb was postulated to play a

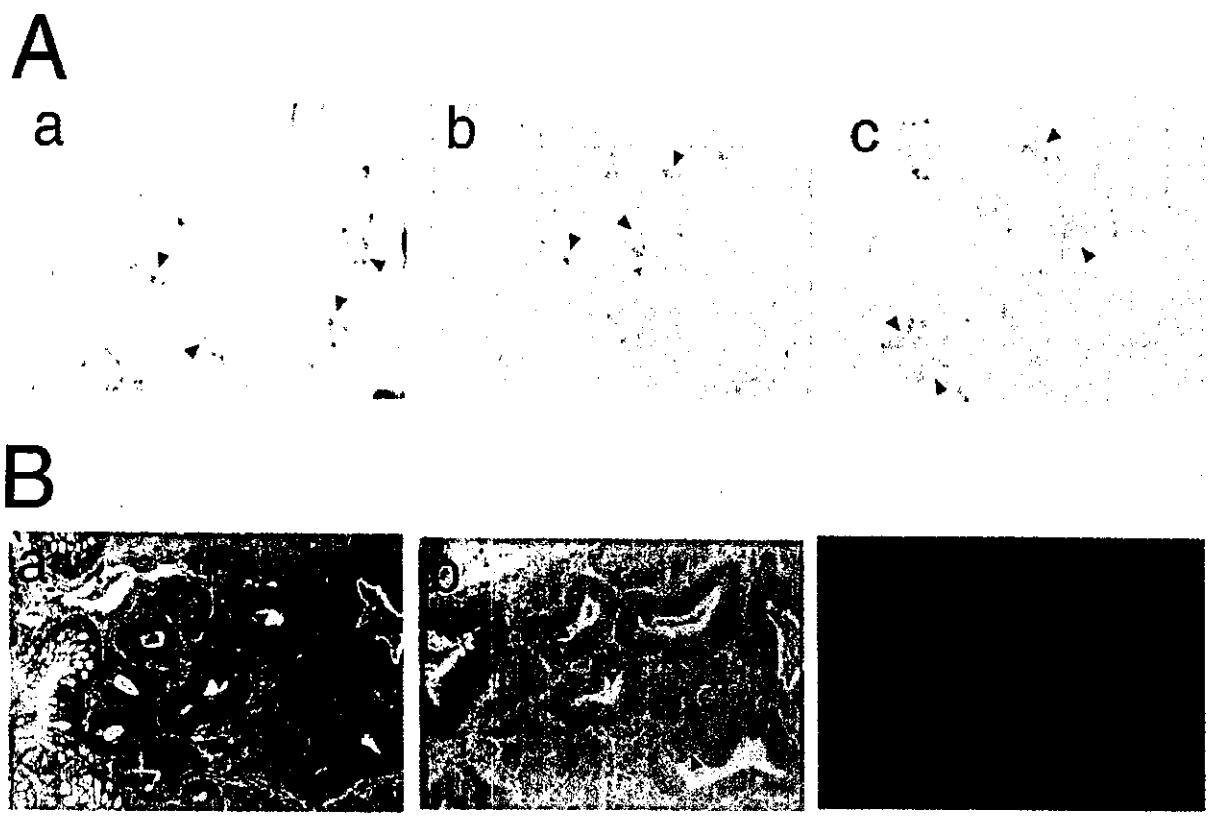

Fig. 3. Histological analysis of colon cancer tissues. (A) Frozen tissue sections were subjected to AB-PAS staining (a) and *in situ* hybridization with a *defensin NP3* (b) or *defensin 5* probe (c). Arrowheads in (b) and (c) indicate cells with *defensin NP3* and *defensin 5* transcripts, respectively. (B) Serial sections of paraffin embedded colon cancer tissues were subjected to H&E staining (a), AB-PAS staining (b) and immunostaining with an anti-lysozyme IgG antibody (c). As arrowheads indicate, Paneth cells can be recognized by the presence of typical pink granules (Paneth granules) by H&E staining. Paneth granules are also clearly visualized by AB-PAS staining (b) and by immunostaining for lysozyme protein (c).

central role (41). The results indicate that the molecular basis underlying PhIP carcinogenesis could differ from organ to organ, although cell proliferation may be accelerated by PhIP in both cases. In fact, β-catenin mutations are frequently observed in rat colon cancers (11–13), but only rarely in mammary tumors (42). Moreover, the mutation spectra found in PhIP-induced tumors also differ with the organ (43).

It is of great interest to note that Paneth cells were observed in colon cancers and even in much earlier lesions, dysplastic ACF. Paneth cells exist mainly in the small intestine and sometimes in colonic tumors, but are rarely found in normal colon epithelium (44,45). Yamada *et al.* have recently reported the presence of Paneth cells in crypts which accumulated β-catenin (BCAC) induced by an alkylating agent, azoxymethane (46,47). Based on their observations and a previous report by Wilson *et al.* (48), Yamada and Mori (49) suggested a dysdifferentiating potential of BCAC and that Paneth cell differentiation could promote intestinal carcinogenesis. Taking the results together, the appearance of Paneth cells in colon cancers does not appear to be carcinogen-specific, but could be a common phenomenon in the development of colon cancers. Although the molecular mechanisms underlying the induction of Paneth cells in colon cancers remain to be clarified, activation of the Wnt/Apc/β-catenin signaling pathway could be one causative event. Inhibition of β-catenin/TCF signaling in colon cancer cell lines indeed results in G_1 arrest or induction of markers which are characteristic of differentiated colon epithelial cells, as described previously (50). Mice deficient for the TCF4 transcription factor completely lack proliferating cells in the fetal small intestinal epithelium (51). The Wnt/APC/β-catenin signaling pathway thus could be essential for maintenance of the differentiated or undifferentiated status of intestinal epithelial cells. Activation of the Wnt/APC/β-catenin pathway may therefore affect the differentiation process and induce dysdifferentiation of colon epithelial cells as a consequence. Activation of this pathway is commonly observed in both PhIP- (10–15) and azoxymethane-induced (35,52,53) colon cancers and also in preneoplastic lesions (15). Gene expression analysis of teratomas, derived from embryonic stem cells with null APC, showed up-regulation of *defensin* α genes compared with teratomas derived from embryonic stem cells with wild-type APC (54). Paneth cells were also observed in APC-deficient teratoma tissues (54). Again, it is highly plausible that activation of the Wnt/APC/β-catein signaling pathway is a genetic causation of Paneth cell differentiation in colon cancer tissues. Although the biological consequences of Paneth cell differentiation (or metaplasia) for colon carcinogenesis remain to be clarified, it is

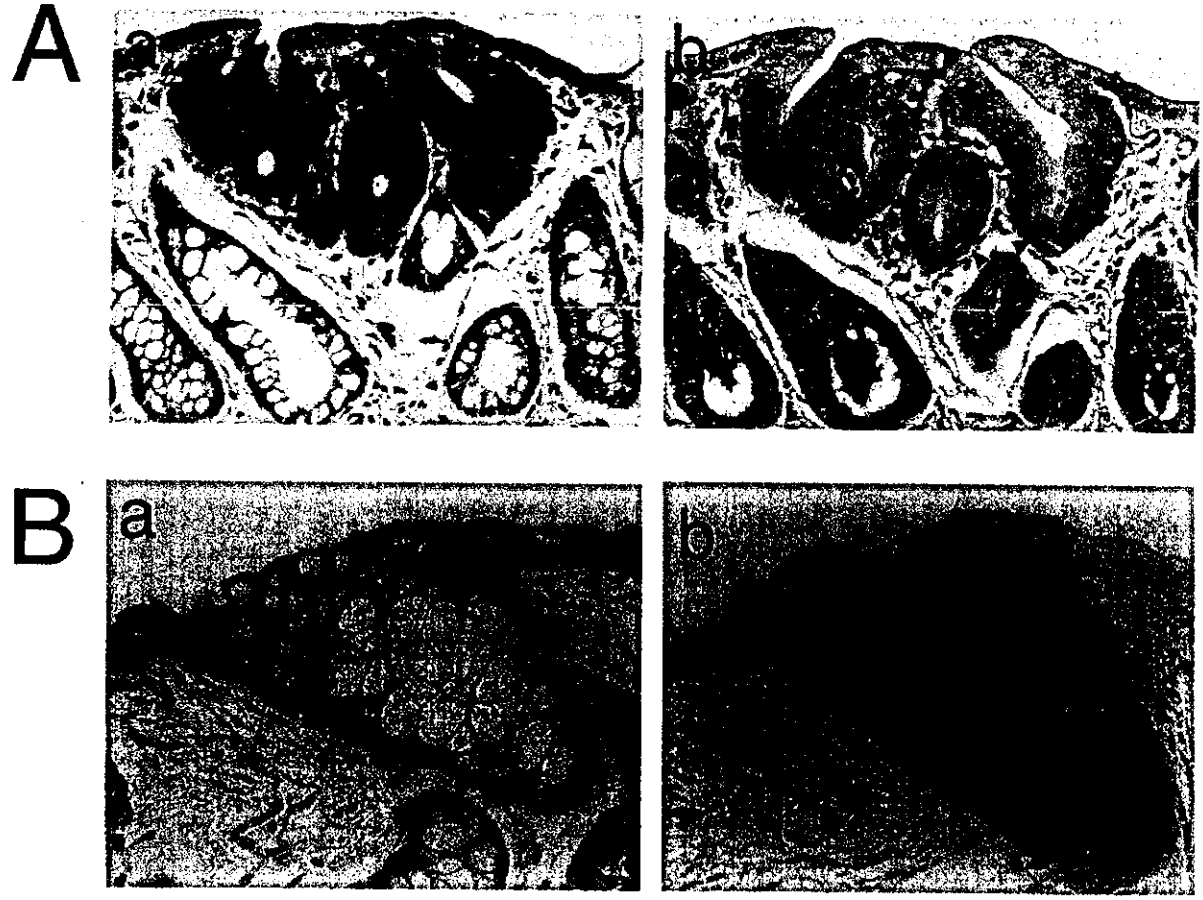

Fig. 4. Histological analysis of ACF. Serial sections of paraffin embedded high grade dysplastic (A) and non-dysplastic ACF (B) observed at experimental week 18. AB-PAS-positive Paneth granules are clearly evident in the high grade dysplastic ACF, but not in the non-dysplastic lesion. Another high grade dysplastic ACF collected at week 25 also gave similar results (data not shown). (a) H&E staining; (b) AB-PAS staining.

possible that the appearance of Paneth cells reflects aberrant differentiation of colonic stem cells. Whatever the case, defensin could be utilized as a potential serological marker for early detection of colon cancers because of its nature as a secreted molecule.

Acknowledgements

This work was supported in part by a Grant-in-Aid for the Second Term of the Comprehensive 10-Year Strategy for Cancer Control from the Ministry of Health, Labour and Welfare of Japan, and by a Grant-in-Aid for Scientific Research on Priority Areas of Cancer from the Ministry of Education, Science, Sport, Culture and Technology of Japan. K.F. was the recipient of a Research Resident Fellowship from the Foundation for Promotion of Cancer Research in Japan while this work was being conducted.

References

1. Chung,D.C. (2000) The genetic basis of colorectal cancer: insights into critical pathways of tumorigenesis. *Gastroenterology*, **119**, 854–865.
2. Kinzler,K.W. and Vogelstein,B. (2002) Colorectal tumors. In Kinzler K.W. and Vogelstein B. (eds), *The Genetic Basis of Human Cancer*. McGraw-Hill, New York, NY, pp. 583–612.
3. Felton,J.S., Knize,M.G., Shen,N.H., Lewis,P.R., Andresen,B.D., Happe,J. and Hatch,F.T. (1986) The isolation and identification of a new mutagen from fried ground beef: 2-amino-1-methyl-6-phenylimidazo[4,5-*b*]pyridine (PhIP). *Carcinogenesis*, **7**, 1081–1086.
4. Wakabayashi,K., Nagao,M., Esumi,H. and Sugimura,T. (1992) Food-derived mutagens and carcinogens. *Cancer Res.*, **52**, 2092s–2098s.
5. Takahashi,S., Ogawa,K., Ohshima,H., Esumi,H., Ito,N. and Sugimura,T. (1991) Induction of aberrant crypt foci in the large intestine of F344 rats by oral administration of 2-amino-1-methyl-6-phenylimidazo[4,5-*b*]pyridine. *Jpn. J. Cancer Res.*, **82**, 135–137.
6. Ochiai,M., Nakagama,H., Watanabe,M., Ishiguro,Y., Sugimura,T. and Nagao,M. (1996) Efficient method for rapid induction of aberrant crypt foci in rats with 2-amino-1-methyl-6-phenylimidazo[4,5-*b*]pyridine. *Jpn. J. Cancer Res.*, **87**, 1029–1033.
7. Bird,R.P. (1987) Observation and quantification of aberrant crypts in the murine colon treated with a colon carcinogen: preliminary findings. *Cancer Lett.*, **37**, 147–151.
8. McLellan,E.A. and Bird,R.P. (1988) Aberrant crypts: potential preneoplastic lesions in the murine colon. *Cancer Res.*, **48**, 6187–6192.
9. Ito,N., Hasegawa,R., Sano,M., Tamano,S., Esumi,H., Takayama,S. and Sugimura,T. (1991) A new colon and mammary carcinogen in cooked food, 2-amino-1-methyl-6-phenylimidazo[4,5-*b*]pyridine (PhIP). *Carcinogenesis*, **12**, 1503–1506.
10. Kakiuchi,H., Watanabe,M., Ushijima,T., Toyota,M., Imai,K., Weisburger,J.H., Sugimura,T. and Nagao,M. (1995) Specific 5′-GGGA-3′ > 5′-GGA-3′ mutation of the Apc gene in rat colon tumors induced by 2-amino-1-methyl-6-phenylimidazo[4,5-*b*]pyridine. *Proc. Natl Acad. Sci. USA*, **92**, 910–914.

11. Dashwood,R.H., Suzui,M., Nakagama,H., Sugimura,T. and Nagao,M. (1998) High frequency of β-catenin (*ctnnb1*) mutations in the colon tumors induced by two heterocyclic amines in the F344 rat. *Cancer Res.*, **58**, 1127–1129.
12. Tsukamoto,T., Tanaka,H., Fukami,H., Inoue,M., Takahashi,M., Wakabayashi,K. and Tatematsu,M. (2000) More frequent beta-catenin gene mutations in adenomas than in aberrant crypt foci or adenocarcinomas in the large intestines of 2-amino-1-methyl-6-phenylimidazo[4,5-*b*]pyridine (PhIP)-treated rats. *Jpn. J. Cancer Res.*, **91**, 792–796.
13. Ubagai,T., Ochiai,M., Kawamori,T., Imai,H., Sugimura,T., Nagao,M. and Nakagama,H. (2002) Efficient induction of rat large intestinal tumors with a new spectrum of mutations by intermittent administration of 2-amino-1-methyl-6-phenylimidazo[4,5-*b*]pyridine in combination with a high fat diet. *Carcinogenesis*, **23**, 197–200.
14. Nakagama,H., Ochiai,M., Ubagai,T., Tajima,R., Fujiwara,K., Sugimura,T. and Nagao,M. (2002) A rat colon cancer model induced by 2-amino-1-methyl-6-phenylimidazo[4,5-*b*]pyridine, PhIP. *Mutat. Res.*, **506/507**, 137–144.
15. Ochiai,M., Ushigome,M., Fujiwara,K., Ubagai,T., Kawamori,T., Sugimura,T., Nagao,M. and Nakagama,H. (2003) Characterization of dysplastic aberrant crypt foci in the rat colon induced by 2-amino-1-methyl-6-phenylimidazo[4,5-*b*]pyridine. *Am. J. Pathol.*, **163**, 1607–1614.
16. Hoshino,M., Sone,M., Fukata,M., Kuroda,S., Kaibuchi,K., Nabeshima,Y. and Hama,C. (1999) Identification of the stef gene that encodes a novel guanine nucleotide exchange factor specific for Rac1. *J. Biol. Chem.*, **247**, 17837–17844.
17. Yoshida,S., Ohbo,K., Takakura,A., Takebayashi,H., Okada,T., Abe,K. and Nabeshima,Y. (2001) Sgn1, a basic helix–loop–helix transcription factor delineates the salivary gland duct cell lineage in mice. *Dev. Biol.*, **240**, 517–530.
18. Fujiwara,K., Ochiai,M., Ubagai,T., Ohki,M., Ohta,T., Nagao,M., Sugimura,T. and Nakagama,H. (2003) Differential gene expression profiles in colon epithelium of two rat strains with distinct susceptibility to colon carcinogenesis after exposure to PhIP in combination with dietary high fat. *Cancer Sci.*, **94**, 672–678.
19. Dragani,T.A., Manenti,G., Della Porta,G., Gattoni-Celli,S. and Weinstein,I.B. (1986) Expression of retroviral sequences and oncogenes in murine hepatocellular tumors. *Cancer Res.*, **46**, 1915–1919.
20. van der Houven van Oordt,C.W., Schouten,T.G., van der Eb,A.J. and Breuer,M.L. (1999) Differentially expressed transcripts in X-ray-induced lymphomas identified by dioxygenin-labeled differential display. *Mol. Carcinog.*, **24**, 29–35.
21. Ouellette,A.J., Hsieh,M.M., Nosek,M.T., Cano-Gauci,D.F., Huttner,K.M., Buick,R.N. and Selsted,M.E. (1994) Mouse Paneth cell defensins: primary structures and antibacterial activities of numerous cryptdin isoforms. *Infect. Immun.*, **62**, 5040–5047.
22. Yount,N.Y., Wang,M.S., Yuan,J., Banaiee,N., Ouellette,A.J. and Selsted,M.E. (1995) Rat neutrophil defensins. Precursor structures and expression during neutrophilic myelopoiesis. *J. Immunol.*, **155**, 4476–4484.
23. Ouellette,A.J. (1997) Paneth cells and innate immunity in the crypt microenvironment. *Gastroenterology*, **113**, 1779–1784.
24. Notterman,D.A., Alon,U., Sierk,A.J. and Levine,A.J. (2001) Transcriptional gene expression profiles of colorectal adenoma, adenocarcinoma and normal tissue examined by oligonucleotide arrays. *Cancer Res.*, **61**, 3124–3130.
25. Buckhaults,P., Rago,C., St Croix,B., Romans,K.E., Saha,S., Zhang,L., Vogelstein,B. and Kinzler,K.W. (2001) Secreted and cell surface genes expressed in benign and malignant colorectal tumors. *Cancer Res.*, **61**, 6996–7001.
26. McDonnell,S., Navre,M., Coffey,R.J.,Jr and Matrisian,L.M. (1991) Expression and localization of the matrix metalloproteinase pump-1 (MMP-7) in human gastric and colon carcinomas. *Mol. Carcinog.*, **4**, 527–533.
27. Yoshimoto,M., Itoh,F., Yamamoto,H., Hinoda,Y., Imai,K. and Yachi,A. (1993) Expression of MMP-7 (PUMP-1) mRNA in human colorectal cancers. *Int. J. Cancer*, **54**, 614–618.
28. Kennedy,B.P., Soravia,C., Moffat,J., Xia,L., Hiruki,T., Collins,S., Gallinger,S. and Bapat,B. (1998) Overexpression of the nonpancreatic secretory group II PLA2 messenger RNA and protein in colorectal adenomas from familial adenomatous polyposis patients. *Cancer Res.*, **58**, 500–503.
29. Bartkova,J., Thullberg,M., Slezak,P., Jaramillo,E., Rubio,C., Thomassen,L.H. and Bartek,J. (2001) Aberrant expression of G1-phase cell cycle regulators in flat and exophytic adenomas of the human colon. *Gastroenterology*, **120**, 1680–1688.
30. Cooper,E.H., Turner,R., Geekie,A., Neville,A.M., Goligher,J.C., Graham,N.G., Giles,G.R., Hall,R. and Macadam,W.A. (1976) Alpha-globulins in the surveillance of colorectal cancer. *Biomedicine*, **24**, 171–178.
31. Claeskens,A., Ongenae,N., Neefs,J.M., Cheyns,P., Kaijen,P., Cools,M. and Kutoh,E. (2000) Hevin is down-regulated in many cancers and is a negative regulator of cell growth and proliferation. *Br. J. Cancer*, **82**, 1123–1130.
32. Birkenkamp-Demtroder,K., Christensen,L.L., Olesen,S.H., Frederiksen,C.M., Laiho,P., Aaltonen,L.A., Laurberg,S., Sorensen,F.B., Hagemann,R. and ORntoft,T.F. (2002) Gene expression in colorectal cancer. *Cancer Res.*, **62**, 4352–4363.
33. Ganz,T. (1999) Defensins and host defense. *Science*, **286**, 420–421.
34. Mallow,E.B., Harris,A., Salzman,N., Russell,J.P., DeBerardinis,R.J., Ruchelli,E. and Bevins,C.L. (1996) Human enteric defensins. Gene structure and developmental expression. *J. Biol. Chem.*, **271**, 4038–4045.
35. Takahashi,M., Fukuda,K., Sugimura,T. and Wakabayashi,K. (1998) β-catenin is frequently mutated and demonstrates altered cellular location in azoxymethane-induced rat colon tumors. *Cancer Res.*, **58**, 42–46.
36. Ho,S.B., Niehans,G.A., Lyftogt,C., Yan,P.S., Cherwitz,D.L., Gum,E.T., Dahiya,R. and Kim,Y.S. (1993) Heterogeneity of mucin gene expression in normal and neoplastic tissues. *Cancer Res.*, **53**, 641–651.
37. Velcich,A., Yang,W., Heyer,J., Fragale,A., Nicholas,C., Viani,S., Kucherlapati,R., Lipkin,M., Yang,K. and Augenlicht,L. (2002) Colorectal cancer in mice genetically deficient in the mucin Muc2. *Science*, **295**, 1726–1729.
38. Ushijima,T., Kakiuchi,H., Makino,H., Hasegawa,R., Ishizaka,Y., Hirai,H., Yazaki,Y., Ito,N., Sugimura,T. and Nagao,M. (1994) Infrequent mutation of Ha-ras and p53 in rat mammary carcinomas induced by 2-amino-1-methyl-6-phenylimidazo[4,5-*b*]pyridine. *Mol. Carcinog.*, **10**, 38–44.
39. Makino,H., Ushijima,T., Kakiuchi,H., Onda,M., Ito,N., Sugimura,T. and Nagao,M. (1994) Absence of p53 mutations in rat colon tumors induced by 2-amino-6-methyldipyrido[1,2-a:3′,2′-*d*]imidazole, 2-amino-3-methylimidazo[4,5-f]quinoline, or 2-amino-1-methyl-6-phenylimidazo]4,5-*b*]pyridine. *Jpn. J. Cancer Res.*, **85**, 510–514.
40. Shan,L., He,M., Yu,M., Qiu,C., Lee,N.H., Liu,E.T. and Snyderwine,E.G. (2002) cDNA microarray profiling of rat mammary gland carcinomas induced by 2-amino-1-methyl-6-phenylimidazo[4,5-*b*]pyridine and 7,12-dimethylbenz[*a*]anthracene. *Carcinogenesis*, **23**, 1561–1568.
41. Qiu,C., Shan,L., Yu,M. and Snyderwine,E.G. (2003) Deregulation of the cyclin D1/Cdk4 retinoblastoma pathway in rat mammary gland carcinomas induced by the food-derived carcinogen 2-amino-1-methyl-6-phenylimidazo[4,5-*b*]pyridine. *Cancer Res.*, **63**, 5674–5678.
42. Yu,M., Ryu,D.Y. and Snyderwine,E.G. (2000) Genomic imbalance in rat mammary gland carcinomas induced by 2-amino-1-methyl-6-phenylimidazo(4,5-*b*)pyridine. *Mol. Carcinog.*, **27**, 76–83.
43. Okochi,E., Watanabe,N., Shimada,Y., Takahashi,S., Wakazono,K., Shirai,T., Sugimura,T., Nagao,M. and Ushijima,T. (1999) Preferential induction of guanine deletion at 5′-GGGA-3′ in rat mammary glands by 2-amino-1-methyl-6-phenylimidazo[4,5-*b*]pyridine. *Carcinogenesis*, **20**, 1933–1938.
44. Shousha,S. (1979) Paneth cell-rich papillary adenocarcinoma and a mucoid adenocarcinoma occurring synchronously in colon: a light and electron microscopic study. *Histopathology*, **3**, 489–501.
45. Pai,M.R., Coimbatore,R.V. and Naik,R. (1998) Paneth cell metaplasia in colonic adenocarcinoms. *Indian J. Cancer*, **35**, 38–41.
46. Yamada,Y., Yoshimi,N., Hirose,Y., Matsunaga,K., Katayama,M., Sakata,K., Shimizu,M., Kuno,T. and Mori,H. (2001) Sequential analysis of morphological and biological properties of beta-catenin-accumulated crypts, provable premalignant lesions independent of aberrant crypt foci in rat colon carcinogenesis. *Cancer Res.*, **61**, 1874–1878.
47. Hirose,Y., Kuno,T., Yamada,Y., Sakata,K., Katayama,M., Yoshida,K., Qiao,Z., Hata,K., Yoshimi,N. and Mori,H. (2003) Azoxymethane-induced beta-catenin-accumulated crypts in colonic mucosa of rodents as an intermediate biomarker for colon carcinogenesis. *Carcinogenesis*, **24**, 107–111.
48. Wilson,C.L., Ouellette,A.J., Satchell,D.P., Ayabe,T., Lopez-Boado,Y.S., Stratman,J.L., Hultgren,S.J., Matrisian,L.M. and Parks,W.C. (1999) Regulation of intestinal α-defensin activation by the metalloproteinase matrilysin in innate host defense. *Science*, **286**, 113–117.
49. Yamada,Y. and Mori,H. (2003) Pre-cancerous lesions for colorectal cancers in rodents: a new concept. *Carcinogenesis*, **24**, 1015–1019.

50. van de Wetering,M., Sancho,E., Verweij,C. *et al.* (2002) The beta-catenin/TCF-4 complex imposes a crypt progenitor phenotype on colorectal cancer cells. *Cell*, **111**, 241–250.
51. Korinek,V., Barker,N., Moerer,P., van Donselaar,E., Huls,G., Peters,P.J. and Clevers,H. (1998) Depletion of epithelial stem-cell compartments in the small intestine of mice lacking Tcf-4. *Nature Genet.*, **19**, 379–383.
52. Sheng,H., Shao,J., Williams,C.S., Pereira,M.A., Taketo,M.M., Oshima,M., Reynolds,A.B., Washington,M.K., DuBois,R.N. and Beauchamp,R.D. (1998) Nuclear translocation of β-catenin in hereditary and carcinogen-induced intestinal adenomas. *Carcinogenesis*, **19**, 543–549.
53. Takahashi,M., Nakatsugi,S., Sugimura,T. and Wakabayashi,K. (2000) Frequent mutations of the β-catenin gene in mouse colon tumors induced by azoxymethane. *Carcinogenesis*, **21**, 1117–1120.
54. Kielman,M.F., Rindapaa,M., Gaspar,C., van Poppel,N., Breukel,C., van Leeuwen,S., Taketo,M.M., Roberts,S., Smits,R. and Fodde,R. (2002) Apc modulates embryonic stem-cell differentiation by controlling the dosage of β-catenin signaling. *Nature Genet.*, **32**, 594–605.

Received October 24, 2003; revised March 11, 2004; accepted March 22, 2004

The Pharmacogenomics Journal (2004) 4, 114–126

www.nature.com/tpj

ORIGINAL ARTICLE

Comprehensive expression analysis of a rat depression model

N Nakatani[1]
H Aburatani[1,2]
K Nishimura[3]
J Semba[1,4]
T Yoshikawa[1]

[1]*Laboratory for Molecular Psychiatry, RIKEN Brain Science Institute, Wako, Saitama, Japan;* [2]*Department of Cancer Systems Biology, Research Center for Advanced Science and Technology, The University of Tokyo, Tokyo, Japan;* [3]*Department of Information Systems, Research Center for Advanced Science and Technology, The University of Tokyo, Tokyo, Japan;* [4]*The University of the Air, Chiba, Japan*

Correspondence:
Dr T Yoshikawa, Laboratory for Molecular Psychiatry, RIKEN Brain Science Institute, 2-1 Hirosawa, Wako, Saitama 351-0198, Japan.
Tel: +81 48 467 5968
Fax: +81 48 467 7462
E-mail: takeo@brain.riken.go.jp

Received: 20 May 2003
Revised: 03 November 2003
Accepted: 10 December 2003

ABSTRACT

Herein we report on a large-scale analysis of gene expression in the 'learned helplessness' (LH) rat model of human depression, using DNA microarrays. We compared gene expression in the frontal cortex (FC) and hippocampus (HPC) of untreated controls, and LH rats treated with saline (LH-S), imipramine or fluoxetine. A total of 34 and 48 transcripts were differentially expressed in the FC and HPC, respectively, between control and LH-S groups. Unexpectedly, only genes for NADH dehydrogenase and zinc transporter were altered in both the FC and HPC, suggesting limited overlap in the molecular processes from specific areas of the brain. Principal component analysis revealed that sets of upregulated metabolic enzyme genes in the FC and downregulated genes for signal transduction in the HPC can distinguish clearly between depressed and control animals, as well as explain the responsiveness to antidepressants. This comprehensive data could help to unravel the complex genetic predispositions involved in human depression.
The Pharmacogenomics Journal (2004) 4, 114–126. doi:10.1038/sj.tpj.6500234

Keywords: learned helplessness; DNA microarray; frontal cortex; hippocampus; antidepressant

INTRODUCTION

Depression is a complex psychiatric disease with specific symptoms that include depressed mood, loss of interest, diminished appetite, sleep disturbances and psychomotor retardation. Depression is common, with lifetime prevalence estimated to be up to 20%,[1] and the condition exacts high personal and social costs on sufferers. The illness is also a major cause of suicide. Epidemiological studies suggest a genetic component to affective disorder,[1,2] and efforts to identify susceptibility genes by linkage and other genetic analyses are being conducted.[3] However, the precise etiologies remain elusive, as does the development of new therapies against depression, particularly for cases that are refractory to conventional therapy. In the case of complex trait diseases, isolating genetic mechanisms using human disease material is often difficult because of sample heterogeneity and other confounding factors. Analysis of suitable animal models under strictly controlled conditions would therefore be beneficial.

To investigate the molecular basis of depression, we have applied DNA microarray technology to analyze gene expressions in learned helplessness (LH) rats, an animal model of depression. After pretreatment with repeated inescapable shocks, animals with LH display decreased ability to escape adverse situations. This behavioral model was originally described in dogs,[4] and later analogous behavior was induced in rats.[5] LH animals display behavioral phenotypes resembling human depressive symptoms, and LH can be ameliorated

using antidepressant drugs.[6,7] LH therefore fulfills the parameters of construct validity, face validity and predictive validity,[8] confirming the suitability of the model for studying the neurobiology of depressive illness and the actions of antidepressants.[9–11] It is also important to note that the 'depressive state' in LH animals lasts for over 3 weeks,[12] making this model particularly useful for studying the chronic changes in brain physiology that accompany depression. We examined the frontal cortex (FC) and hippocampus (HPC) of LH rats, because positron emission tomography scanning and functional magnetic resonance imaging studies have recently indicated a potential abnormality in the frontal cortex of both familial bipolar and unipolar depressives.[13] In addition, recent evidence has suggested that neurogenesis in the HPC may be disturbed in depressive patients.[14–16]

In this study, we have analyzed brain transcripts altered during LH and followed their responsiveness to a classical tricyclic antidepressant (TCA), imipramine, and a new generation selective serotonin reuptake inhibitor (SSRI), fluoxetine. In addition, we performed principal component analysis (PCA) to extract essential gene sets from complex expression data sets that can best explain the different pathophysiological conditions. This was achieved by considering genes as variables in PCA. When genes are variables, the analysis creates a set of principal gene components indicating the features of genes that best explain the experimental responses. Using these comprehensive pharmaco-behavioral genetic approaches, we have attempted to generate data that would eventually allow for the formulation of hypotheses to help understand the molecular and genetic pathophysiology of depression. This in turn could lead to the development of novel antidepressants with greater efficacy.

RESULTS AND DISCUSSION

Effectiveness of Antidepressants in Learned Helplessness

The LH model is difficult to generate, requiring meticulous refinement of multiple experimental parameters. In our experimental setting, after inescapable shock pretreatment, animals were subjected to 15 avoidance trials at 30 s intervals. In each trial, a current was applied via the floor grid during the first 3 s. If an animal moved to a neighboring compartment within this period (escape response), the shock was terminated. Failures in escape response were counted as a measure of LH. We defined animals as being in a state of LH when escape failures were demonstrated in more than half of the trials in the session. Using this system, we reproducibly induced LH in rats with a success rate of ~40%. LH rats were subsequently treated with repeated injections of saline (LH-S), fluoxetine (LH-F) or imipramine (LH-I), then re-evaluated for escape responses in the test session. Figure 1 shows a schematic of these procedures. During the escapable shock of the test session, all animals in the LH-S group ($n=10$) showed more than eight escape failures, and the mean failure was significantly higher than that of control rats (those that were not given inescapable shock, $n=15$) (Figure 2). Antidepressant administration significantly reduced the number of escape failures for both LH-F ($P<0.05$) and LH-I ($P<0.01$). Imipramine recovered all

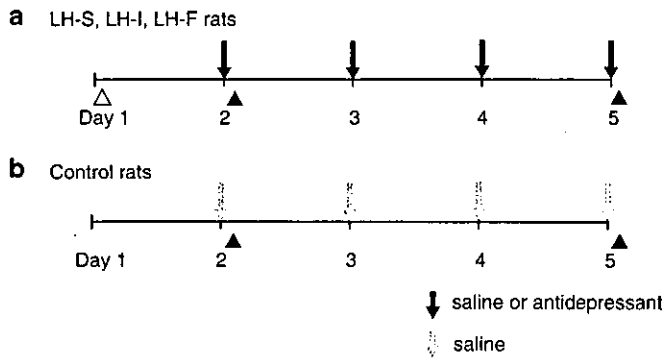

Figure 1 Schematic representation of behavioral procedures. (a) To induce the LH state, animals were given inescapable shock (△) on day 1. On day 2, they received escapable shock (▲), and were selected as 'LH rats' if they showed greater than 50% failure in escape responses. LH animals were then administered saline (LH-S) or antidepressants (LH-F, LH-I) for 4 consecutive days. These animals received escapable shock (▲) again on day 5 to determine whether they were still in the LH state. (b) Control rats were not given inescapable shock on day 1, but treated in the same way thereafter as the LH rats.

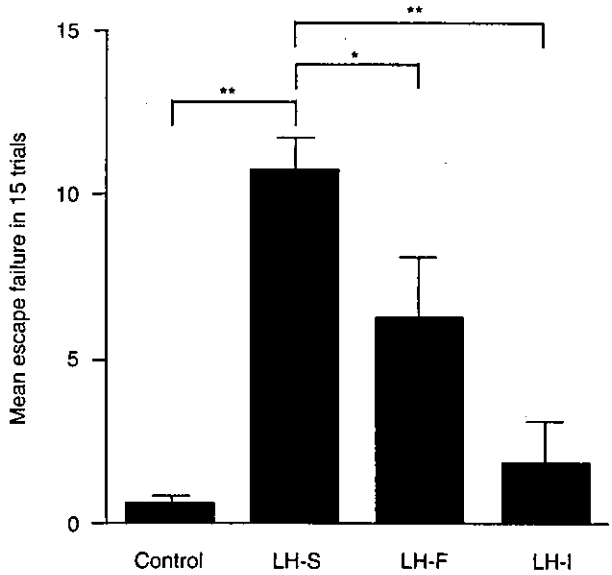

Figure 2 Mean number of escape failures (±SE) during the 15 avoidance trials. Controls ($n=15$) were not given inescapable shocks. Rats exposed to prior inescapable shocks were treated with saline (LH-S) ($n=10$), fluoxetine (LH-F) ($n=7$) or imipramine (LH-I) ($n=9$) once a day for consecutive days (days 2–5). Escape failure refers to the failure of animals to move into the safe compartment during electric footshock (0.5 mA, 3 s duration). The mean numbers of escape failures among groups were evaluated by ANOVA, $F(3,37)=23.69$. $^*P<0.01$ and $^{**}P<0.001$ by *post hoc* Tukey–Kramer test.

rats from the LH state ($n=9$), and fluoxetine reinstated five out of seven. These results confirm the persistency of LH in our animals and the effectiveness of antidepressants in this model.[5,17–20] Fluoxetine produced a weaker response compared to imipramine in alleviating the LH phenotype (Figure 2). We also tested larger doses of each drug, 10 mg/kg i.p. of fluoxetine and 50 mg/kg i.p. of imipramine, but did not observe any significant change in the number of escape failures (10 mg/kg of fluoxetine, 5.0 ± 1.0 ($n=3$); 50 mg/kg of imipramine, 2.0 ± 1.3 ($n=3$)) between the two doses. In addition, Anthony *et al*[21] showed that 5 mg/kg of fluoxetine, the same dose as used in the present study, was enough to elicit monoaminergic perturbation such as a reduced 5-hydroxytryptamine receptor 1B expression in the dorsal raphe of rats. Bristow *et al*[22] also demonstrated the validity and efficacy of 5 mg/kg of fluoxetine in ameliorating depressive behavior in rats. We attempted to minimize the nonspecific effects of the drugs by using the lowest possible dose that maintained antidepressive efficacy.

The present results may reflect the different clinical potencies of the individual agents. TCAs such as imipramine inhibit the reuptake of both serotonin and norepinephrine at nerve terminals by acting on monoamine transporters. In contrast, SSRIs including fluoxetine specifically block the reuptake of serotonin.[2] These differences in pharmacological profiles underlie the distinct antidepressive competences exerted by TCA and SSRI. Although human patients require over 2 weeks of medication before antidepressive effects are observed, we administered the drugs for 4 days in our rodent experiments, in keeping with the protocols of Geoffroy *et al*[6] (5-day treatment) and Tordera *et al*[23] (4-day treatment), and could replicate distinct behavioral responses to therapy.

We also measured weight gain during the 5 days of experiments. Weight increase in the LH-S group was significantly lower than that in controls (LH-S, 18.8 ± 4.4 g; control, 31.7 ± 2.2 g; $P<0.05$).

General Profiles of Gene Expressions Associated with LH and Antidepressant Treatments

We selected six animals each from the control (rats showing no escape failure in the escapable shock session) and LH-S groups, and five each from the LH-F and LH-I groups (these showed $\leqslant 7$ failures in the 15 trials), to perform microarray analyses. Patterns of gene expression in the two brain regions from the four rat groups were examined using the Affymetrix GeneChip U34A, which represents 8799 probe sets and codes over 8000 transcripts including known genes (>5000) and expressed sequence tags (ESTs). Transcript expression from extracted RNA displayed good linearity in both FC and HPC samples (Figure 3). Our stringent criteria identified 34 and 48 transcripts as differentially expressed between control ($n=6$) and LH-S ($n=6$) groups in the FC and HPC, respectively (henceforth referred to as 'LH-associated transcripts') (Figures 3a and b). However, none of these transcripts survived after the Benjamin and Hochbery False Discovery Rate analysis. This observation may confirm the statements of Mirnics *et al*[24] that true gene-expression changes in psychiatric traits are small and

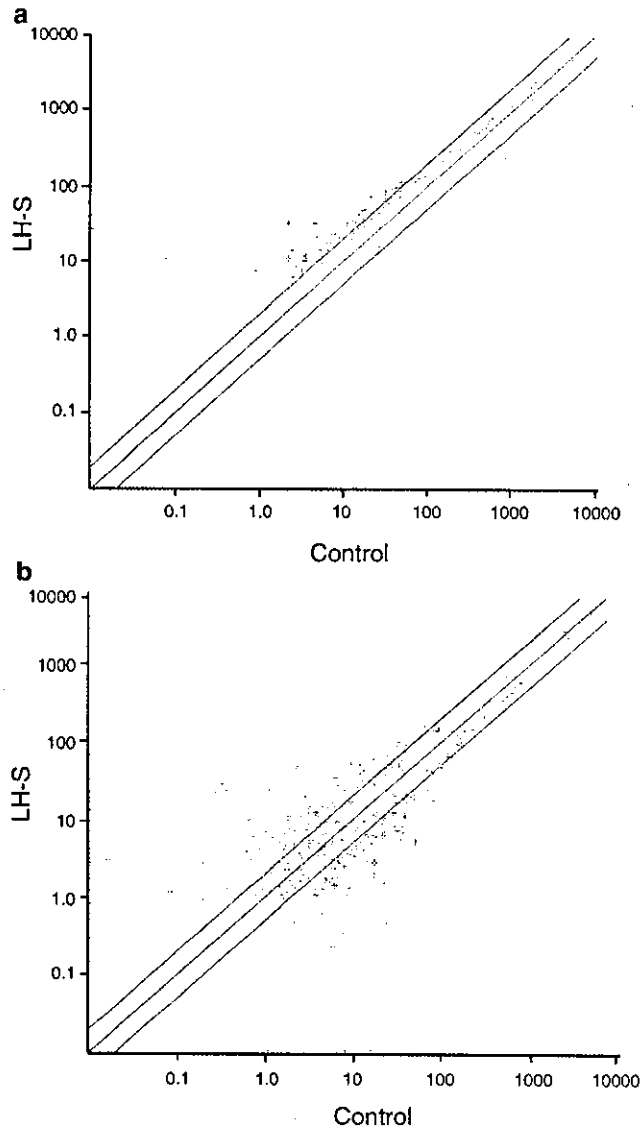

Figure 3 Scatter plot of log-intensity values for the over 8000 genes assayed with the RG-U34A chip in the frontal cortex (a) and hippocampus (b). Each point represents the log value from an average of six control or six LH-S animals.

psychiatric diseases may result from cumulative subtle changes.

Among LH-associated transcripts, five transcripts and one gene showed significant recovery to control levels from the LH state under both imipramine ($n=5$) and fluoxetine ($n=5$) administration in the FC and HPC, respectively (white portions in Figures 4a and b). Transcripts in the pink and yellow areas of Figure 4 represented expression levels that returned to normal after administration of imipramine and fluoxetine, respectively. Interestingly, no LH-associated transcripts demonstrated significant deviation from control levels after drug treatment. That is, none of the LH-associated genes were further decreased or excessively

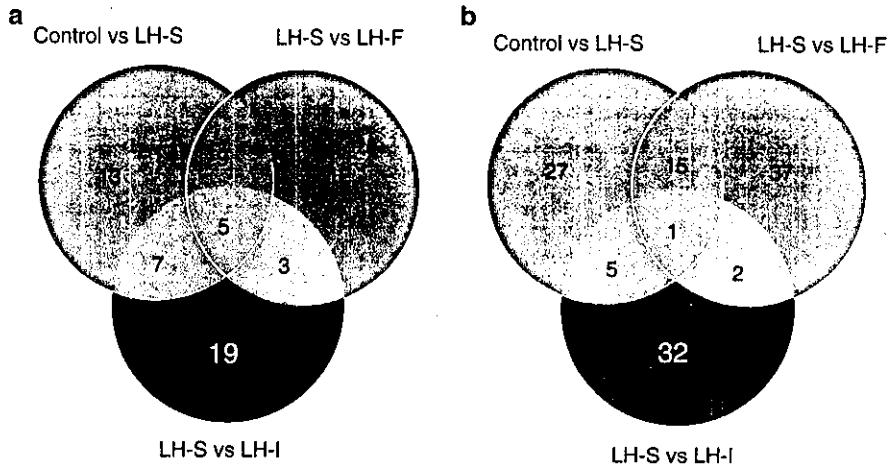

Figure 4 Venn-diagram selection of LH- and antidepressant-associated transcripts in the frontal cortex (a) and hippocampus (b). Comparisons were made between control ($n=6$) and LH-S rats ($n=6$), between LH-S and LH-F rats ($n=5$), and between LH-S and LH-I rats ($n=5$). The LH-I and LH-F rats were those that showed more than 50% success in escape behavior after drug treatments. The number in each compartment denotes the number of differentially expressed transcripts between two groups (see Materials and Methods for a definition of our criteria).

increased after initiating therapy. Approximately 38% of LH-associated transcripts in the FC and 56% in the HPC could not be normalized by either antidepressant (Figure 4; red area). These transcripts could represent the potential targets for novel antidepressants with efficacy against refractory depression. The green, purple and light blue segments in Figure 4 depict the transcripts with expression levels that did not differ between control and LH-S groups, but were significantly altered by fluoxetine, imipramine or both drug treatments, respectively. The information on these transcripts is provided as supplementary Tables S1 and S2. Some of these transcripts may be relevant to the manifestation of adverse reactions by TCA and SSRI. Tables 1 and 2 show the listing of LH-associated transcripts according to putative functions, along with *P*-values between different treatment groups. Data are also provided on the 'average difference'±SE of each transcript (that corresponds to an absolute value) in supplementary Tables S1 and S2. In all, 17 known genes and one EST showed downregulation (marked in red), whereas 16 transcripts including ESTs were upregulated in the FC (Table 1). In contrast, the majority of known LH-associated genes in the HPC were downregulated (27 of 31) (marked in red in Table 2). Even allowing for ESTs, the number of downregulated transcripts in the HPC significantly exceeds the upregulated transcripts (32 *vs* 16) (Table 2).

We chose four genes from each of Tables 1 and 2, and examined mRNA levels in the same RNA samples used for microarray experiments under 'one-step' quantitative RT-PCR reactions (Table 3). These results showed the same direction of expressional changes seen in the microarray experiments, but less correlation was found with the degree of change between the two methods, as indicated in prior studies.[25,26] Furthermore, since only a limited number of transcripts were confirmed by independent methods and no transcripts were confirmed when Bonferroni's correction was applied to the quantitative RT-PCR results, the present DNA microarray data are broadly unconfirmed.

LH-associated Transcripts in the FC

When classified according to function, genes defined as receptors or ion channel/transporters were all downregulated in LH animals (Table 1). Among them, the serotonin receptor type 2A (*Htr2a*) gene showed a 1.6-fold decrease, and recovery with both fluoxetine and imipramine. Evidence from other animal models for depression[27,28] and clinical observations[29] have also suggested a pathological role for *HTR2A* in the depressive state. The change in inositol-1,4,5-triphosphate receptor type 1 (*Itpr1*) level was small, but statistically significant. Both types of antidepressant normalized the reduced expression of *Itpr1*. The observed decrease in both *Htr2a* and *Itpr1* and their restitution to original levels by antidepressants is in keeping with a proposed theory of dysregulated monoamine-mediated calcium signaling in depression.[30,31] Other members of the receptor and ion channel/transporter gene families that showed restoration with fluoxetine or imipramine included a voltage-gated potassium channel and zinc transporter (Table 1). Conversely, three genes from the signal transduction family were all upregulated in LH-S rats compared to controls (Table 1). Of interest is prostaglandin D synthase, an enzyme that produces prostaglandin D_2, a potent endogenous sleep-promoting substance.[32] This enzyme has recently been implicated in the regulation of nonrapid eye movement (NREM).[33] Sleep disturbance is a typical symptom of human depression. Examination of sleep parameters in LH rats, particularly the NREM period, would therefore be of interest. Protein kinase C epsilon (PKCε), which is a member of nPKC, showed a small but significant increase in LH-S compared with controls.

Table 1 LH-associated transcripts in the frontal cortex

Functional Groups	*Fold change*[a]	*P-value*[b]			*Accession no.*
		Cont vs LH-S	*LH-S vs LH-F*	*LH-S vs LH-I*	
Receptor					
Inositol-1,4,5-triphosphate receptor type I	−1.1	0.0032	0.0078	0.0078	J05510
Serotonin receptor 2A	−1.6	0.0479	0.0352	0.0358	M64867
Ion channel/Transporter					
Voltage-gated potassium channel	−1.1	0.0289	0.0078		X62840
Dri 27/ZnT4 (zinc transporter)	−1.3	0.0289		0.0026	Y16774
Cl-/HCO3- exchanger (B3RP2)	−1.4	0.0484			J05166
Signal transduction					
Prostaglandin D2 synthetase	1.3	0.0484	0.0006	0.0181	J04488
PKC epsilon	1.2	0.0158	0.0181		M18331
Neurexophilin 4	2.0	0.0156			AF042714
Neural growth/ structure					
Tau	−1.1	0.0479	0.0358		X79321
Jagged2 precursor	1.3	0.0158		0.0358	U70050
Similar to cdc37	1.6	0.0484			D26564
MAP2	−1.4	0.0158			S74265
H36-alpha7 integrin alpha chain	−1.5	0.0289			X65036
Neu differentiation factor	−1.6	0.0484			M92430
LIMK-1	−9.5	0.0436			D31873
Metabolic enzymes					
Thioradoxin reductase 1	−1.2	0.0011	0.0181		AA891286
F1-ATPase epsilon subunit	1.1	0.0011		0.0026	AI171844
Mitochondrial fumarase	−1.1	0.0110		0.0181	J04473
Lipoprotein lipase	1.5	0.0484			L03294
24-kDa subunit of mitochondrial NADH dehydrogenase	1.4	0.0484			M22756
Bleomycin hydrolase	1.4	0.0158			D87336
Stress response					
Rapamycin and FKBP12 target-1 protein (rRAFT1)	1.1	0.0158	0.0358		U11681
Neuronal death protein	2.3	0.0484			D83697
Poly(ADP-ribose) polymerase	1.6	0.0077			U94340
Others					
Taipoxin-associated calcium binding protein-49 precursor	−1.2	0.0032	0.0119		U15734
Cytosolic resiniferatoxin binding protein RBP-26	−1.3	0.0289	0.0358		X67877
RNA binding protein (transformer-2-like)	−1.2	0.0110	0.0181		D49708
C15	−1.2	0.0002		0.0006	X82445
resection-induced TPI (rs11)	1.4	0.0011			AF007890
Anti-proliferative factor (BTG1)	−1.4	0.0484			L26268
Unknown					
EST	−1.5	0.0158	0.0474	0.0026	AA892280
EST	1.2	0.0484	0.0026		AI230632
EST	1.4	0.0484		0.0078	AA894234
EST	1.2	0.0484		0.0181	AF069782

[a]The fold change was calculated between mean values of control (n = 6) and LH-S rats (n = 6). Positive values indicate an increase, and negative a decrease in gene expression in the LH.
[b]Statistical comparison was made by Mann-Whitney test (two-tailed). Only significant *P*-values (< 0.05) are denoted.

Activation of serotonin 2 receptors reportedly diminished γ-amino butyric acid type A receptor current through PKC in prefrontal cortical neurons.[34] Expression changes in the *Htr2a* and PKCε genes in LH may indicate a functional link between the two systems in the depressive state. The precise role of neurexophilin 4 in the intercellular signaling system remains unclear,[35,36] but the gene may underlie a depression/stress-related physiological pathway that cannot be corrected using TCAs or SSRIs (Table 1).

Of the LH-associated genes identified from the FC, LIMK-1 (LIM domain kinase 1: *Limk1*) displayed the most dramatic decrease, a 9.5-fold reduction compared with control levels (Table 1). Transcriptional levels were not completely normalized by imipramine or fluoxetine treatment. This

Table 2 LH-associated transcripts in the hippocampus

Functional Groups	*Fold change*[a]	*P-value*[b]			*Accession No.*
		Cont vs *LH-S*	*LH-S* vs *LH-F*	*LH-S* vs *LH-I*	
Receptor					
HGL-SL1 olfactory receptor pseudogene	−2.0	0.0005	0.0358		AF091574
olfactory receptor-like protein (SCR D-9)	−1.4	0.0050			AF034899
heparin-binding fibroblast growth factor receptor 2	−2.4	0.0373			L19112
HFV-FD1 olfactory receptor	−2.5	0.0019			AF091575
Ion channel/Transporter					
Dri 27/ZnT4 protein (zinc transporter)	1.2	0.0464	0.0181		Y16774
Chloride channel RCL1	−1.1	0.0373	0.0181		D13985
High-Affinity L-proline transporter	−1.3	0.0050		0.0078	M88111
Plasma membrane CA2+-ATPase isoform 3	−1.4	0.0018			M96626
Signal transduction					
Paranodin	1.2	0.0213	0.0078		AF000114
Arl5 (ADP-ribosylation factor-like 5)	1.4	0.0213			AA956958
Grb14	−1.4	0.0213			AF076619
Neurotransmission					
Synuclein SYN1	−1.2	0.0213	0.0358		S73007
Alpha-soluble NSF attachment protein	−1.1	0.0213		0.0078	X89968
Rab13	−1.9	0.0005		0.0358	M83678
Rab3b	−1.6	0.0213			AA799389
GTP-binding protein (ral B)	−2.0	0.0110			L19699
Neural growth/ structure					
Tuba1 (Alpha-tubulin)	1.2	0.0213	0.0006		AA892548
Zinc-finger protein AT-BP2	−1.4	0.0213			X54250
CRP2 (cysteine-rich protein 2)	−1.4	0.0373			D17512
Nfyb CCAAT binding transcription factor of CBF-B/NFY-B	−1.4	0.0373			AA817843
Decorin	2.2	0.0213			AI639233
Metabolic enzymes					
NADH-cytochrome b-5 reductase	−1.1	0.0110	0.0358	0.0181	AI229440
Siat5 (Sialyltransferase 5)	−1.7	0.0050	0.0078		X76988
24-kDa mitochondrial NADH dehydrogenase precursor	−1.4	0.0373			M22756
2-oxoglutarate carrier	−1.4	0.0110			U84727
Soluble cytochrome b5	−1.5	0.0110			AF007107
Stress response					
Ischemia responsive 94 kDa protein (irp94)	−1.4	0.0050			AF077354
MHC class I antigen	−1.5	0.0373			AF074609
Others					
RNA splicing-related protein	−1.4	0.0373			AI044739
Aes Amino-terminal enhancer of split	−1.4	0.0153			AA875427
Proteasome RN3 subunit	−1.5	0.0110			L17127
Unknown					
EST	1.5	0.0274	0.0358		AA799488
EST	1.4	0.0373	0.0078		AA858617
EST	1.2	0.0213	0.0026		AA892817
EST	1.2	0.0050	0.0026		AA892238
EST	1.1	0.0213	0.0026		AA799893
EST	1.1	0.0050	0.0006		AA799784
EST	−1.5	0.0213	0.0358		AA799525
EST	1.3	0.0373		0.0078	AA893039
EST	−1.1	0.0373		0.0358	AI007820
EST	−1.3	0.0373		0.0358	AA875348
EST	2.4	0.0213			AA875633
EST	1.9	0.0373			AI229655
EST	1.5	0.0373			AA955477
EST	1.5	0.0213			AA893569
EST	1.4	0.0464			AA800803
EST	−1.6	0.0274			AI639477
EST	−1.6	0.0110			AA892353

[a]The fold change was calculated between mean values of control ($n=6$) and LH-S rats ($n=6$). Positive values indicate an increase, and negative values (in red) a decrease in gene expression in the LH.
[b]Statistical comparsion was made by Mann-Whitney test (two-tailed). Only significant *P*-values (<0.05) are denoted.

Table 3 Gene expression levels evaluated by quantitative RT-PCR and comparisons with the results from microarray analysis

	Frontal cortex				*Hippocampus*			
	LIMK-1	*HTR2A*	*PGDS*	*IP3R*	*SNAP*	*SYN1*	*bFGFR2*	*Ca^{2+}-ATPase*
Control	1.00±0.42	1.00±0.57	1.00±0.19	1.00±0.48	1.00±0.36	1.00±0.44	1.00±0.21	1.00±0.31
LH-S	0.49±0.07	0.36±0.06	1.64±0.25[a]	0.97±0.20	0.61±0.14	0.54±0.17	0.88±0.23	0.80±0.37
LH-F	0.50±0.06	0.57±0.26	1.10±0.20	0.52±0.15	0.86±0.14	0.65±0.23	0.65±0.11	0.80±0.14
LH-I	0.44±0.08	0.53±0.08[b]	0.81±0.33	0.72±0.23	1.45±0.51	0.30±0.07	0.52±0.16	0.70±0.29
Fold change evaluated by RT-PCT (Cont *vs* LH-S)	−2.0	−2.8	1.6	−1.0	−1.6	−1.9	−1.1	−1.3
Fold change evaluated by microarray (Cont *vs* LH-S)	−9.5	−1.6	1.3	−1.1	−1.1	−1.2	−2.4	−1.4

The expression level of each gene is normalized to that of the GAPDH gene (mean±SE, $n=6$, each in control and LH-S, $n=5$, each in LH-F and LH-I). The gene abbreviations are: LIMK-1, LIM domain kinase 1; HTR2A, 5-hydroxytryptamine (serotonin) receptor 2A; PGDS, prostaglandin D synthetase; IP3R, inositol-1,4,5-triphosphate receptor type 1; SNAP, synaptosomal-associated protein; SYN1, synuclein 1; bFGFR2, heparin-binding fibroblast growth factor receptor 2; Ca^{2+}-ATPase, plasma membrane Ca^{2+}-ATPase isoform 3.
[a]$P<0.05$ (control *vs* LH-S).
[b]$P<0.05$ (LH-S *vs* LH-I) by Mann–Whitney test (two-tailed).

partial recovery might be due to the low level of normal transcription and the large variation of expression values (supplementary Table S3). We therefore performed real-time RT-PCR to confirm the expression profile of *Limk1*, and detected a two-fold decrease in LH compared to control animals. This reduction was not recovered by antidepressant treatments (Table 3). *Limk1* is expressed in both fetal and adult nervous systems, and shows ubiquitous expression in the brain with the strongest expression in adult cerebral cortex.[37] Recently, *Limk1*-knockout mice were reported to show abnormalities in spine morphology and enhanced long-term potentiation, accompanied by alterations in fear response and spatial learning.[38] A test of depression-related behavioral parameters in these mice would be intriguing. Additional reports that depressive patients frequently manifest subcortical hyperintensity near frontal white matter ('myelin pallor' on histological examination)[39] suggest that LIMK1 may be involved in an as yet undetermined intercellular signaling pathway disrupted in depression, as LIMK1 is known to phosphorylate myelin basic proteins.[40]

Our criteria for selecting 'altered' transcripts in LH compared to control animals may have been conservative and inadvertently excluded many potential candidates. Decreased levels of brain-derived neurotrophic factor (BDNF) recoverable by antidepressant treatment have been reported in patients with depression.[41,42] Although we could not detect any significant difference in expression between control and LH-S animals, we found that expression of BDNF in the FC was increased in LH-I animals compared with LH-S and control animals (supplementary Table S3).

LH-associated Transcripts Specific to the HPC and Common to Both the FC and HPC

In contrast to the FC, most LH-associated genes in the HPC showed decreased expressions on the induction of LH (Table 2). Genes coding for receptors were downregulated in both regions, although there was no overlap between the two groups of receptors. This category included three olfactory receptor-like genes, *HGL-SL1* olfactory pseudogene, olfactory receptor-like protein (*SCRD-9*) and *HFV-FD1* olfactory receptor. Although these are thought to encode G protein-coupled receptors with seven transmembrane domains, the biological functions are unclear. Heparin-binding fibroblast growth factor receptor 2 (*Fgfr2*) genes were also downregulated in LH-S, but were unaffected by antidepressants (Table 2). We also found a reduction in the *N*-methyl-D-aspartate receptor 2A (NMDAR 2A) subunit gene in three of six LH-S animals. Fgfr2 reduces NMDAR 2A subunit mRNA levels via a receptor-mediated mechanism.[43] Chronic administration of antidepressants decreases the expression of NMDA receptor subunit genes and radioligand binding to the receptor.[42] This discrepancy warrants further investigation, to determine the role of this growth factor and the NMDA receptor genes in depression. All the LH-associated genes defined as involved in neurotransmission were also downregulated in this study (Table 2). The hippocampus is well known as a region of the brain that is highly susceptible to stress.[44,45] Recent studies have demonstrated that repeated stress causes shortening and debranching of dendrites in the CA3 region of the HPC and suppresses neurogenesis of granule neurons in the dentate gyrus.[45,46] In addition, chronic antidepressant treatment increases cell populations and neurogenesis in the rat hippocampus.[15] The extensive suppression of gene expression observed in our LH model may be related to phenotypic changes in the hippocampus produced by stress.

An unexpected finding was the scarcity of common transcripts between the two areas of brain. Of the LH-associated genes, only those coding for the 24-kDa mitochondrial NADH dehydrogenase and Dri27/ZnT4 (zinc transporter) were common to both the FC and HPC (Tables 1 and 2). However, the direction of change differed between the two regions. This selectivity was also seen in genes that were not affected by LH, but displayed a response to